Acta Oncologica Symposium
BiGART2010

Biology-Guided Adaptive Radiotherapy

Aarhus - Denmark
May 26-28, 2010

Final programme and abstracts

Welcome!

It is our great pleasure to welcome you to Aarhus, Denmark for the Acta Oncologica symposium on Biology-Guided Adaptive Radiotherapy.

Key topics for the symposium will include:

- Biology of tumours and normal tissue to guide patient selection, target volumes and dose prescription in radiotherapy
- Biological imaging of tumours and normal tissues with functional imaging techniques based on MRI and PET, and the use of such images for dose painting and normal tissue avoidance
- Adaptation of treatment delivery based on changes in tumour and normal tissue biology, anatomy and/or function

The symposium has attracted around 150 physicians, physicists, radiobiologists and other scientists from the Nordic countries and internationally. We look forward to exciting scientific sessions, with presentations from leading scientists from several continents. A considerable number of the studies presented at the meeting are being prepared for publication in the BiGART2010 special issue of the Acta Oncologica journal. We are thankful to both authors and reviewers for this large collective effort that we hope will provide us all with a comprehensive and up-to-date overview of this research area.

All participants and accompanying persons are invited to the social programme. Wednesday evening we have arranged a welcome reception at ARoS Art Museum in Aarhus city. The event includes a guided tour followed by a dinner. Please remember to bring your entrance ticket to ARoS. This ticket will be given to you by check-in or by contacting the registration desk. On Thursday night, the conference dinner will be held at Varna Mansion, a beautifully situated restaurant in the forest next to Hotel Marselis.

We hope you will enjoy the meeting and your time in Aarhus - the “city of smile”!

Ludvig Paul Muren Morten Høyer Jens Overgaard Cai Grau

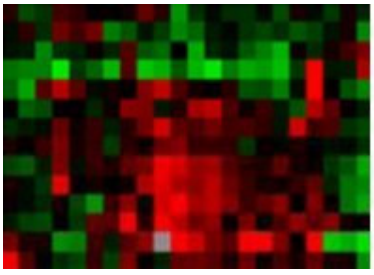
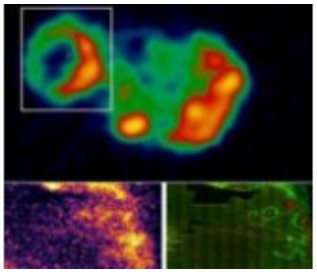
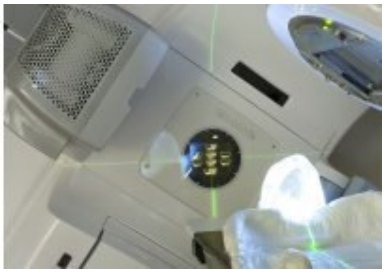

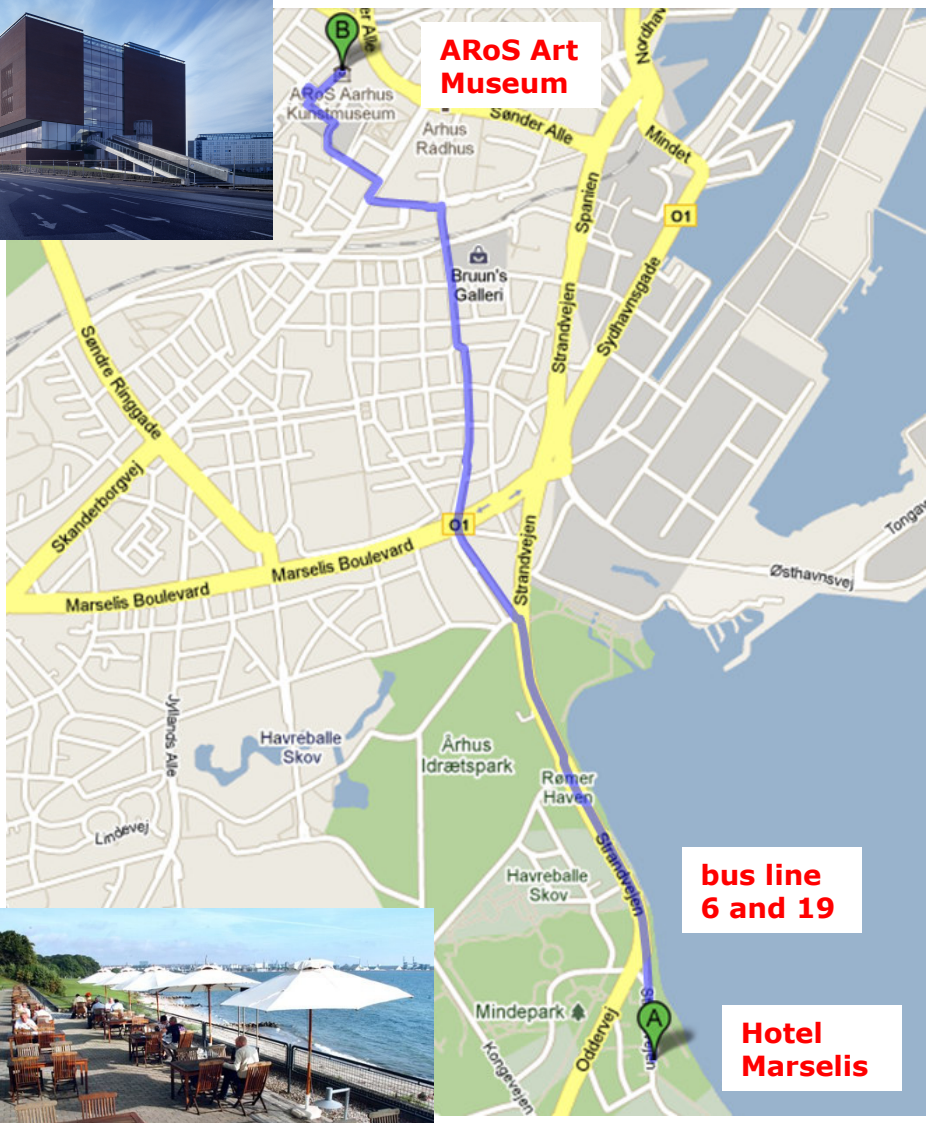
ARoS Art Museum
ARoS Aarhus Kunstmuseum
Århus Rådhus
Sønder Allé
Mindet
Spanien
Bruun's Galleri
Strandvejen
Sydhavnsgade
Søndre Ringgade
Skanderborgvej
Marselis Boulevard
Marselis Boulevard
Østhavnsvej
Jyllands Allé
Havreballe Skov
Århus Idrætspark
Rømer Haven
Havreballe Skov
bus line 6 and 19
Mindepark
Oddervej
Kongevejen
Hotel Marselis

Faculty

Invited speakers

J. Alsner (Aarhus)
H. Bartelink (Amsterdam)
R. Bristow (Toronto)
Y. Cao (Ann Arbor)
S. Combs (Heidelberg)
J. Deasy (St Louis)
M. Fuss (Portland)
V. Gregoire (Brussels)
A. L. Grosu (Freiburg)
K. Haustermans (Leuven)
R. Jeraj (Madison)
M. R. Horsman (Aarhus)
M. Hoyer (Aarhus)
M. Kessler (Ann Arbor)
A. Kjær (Copenhagen)
S. Korreman (Copenhagen/Madison)
P. Lambin (Maastricht)
E. Malinen (Oslo)
H. Nyström (Uppsala)
D.R. Olsen (Oslo)
J. Overgaard (Aarhus)
M. Partridge (Sutton)
R. Pötter (Vienna)
U. van der Heide (Utrecht)
J. Yarnold (Sutton)

Local faculty and organizers

C. Grau (chair, organizing committee)
L. P. Muren (chair, scientific programme)
M. Hoyer (chair, social programme)
J. Overgaard (chair, proceedings)
J. Alsner
N. Bassler
M. Busk
M. R. Horsman
J. C. Lindegaard
T. Nielsen
M. Nordsmark
P. R. Poulsen
B.S. Sørensen
T.S. Sørensen
K. Tanderup

Contact

Prof. Cai Grau
Department of Oncology,
Aarhus University Hospital,
44 Norrebrogade,
DK-8000 Aarhus C
Denmark

Scientific Programme

Wednesday May 26, 2010

13.00-13.05	**Opening of the Symposium** **Cai Grau -** Welcome to BiGART2010 and Aarhus. Practical information
13.05-15.00	**Session 1: Radiobiology** Chairpersons: J. Overgaard and P. Lambin
	Keynote lectures
13.05	**Jens Overgaard, Aarhus:** Clinical radiobiology in Scandinavia
13.25	**Harry Bartelink, Amsterdam:** Individual adaptation of early breast cancer treatment
13.45	**John Yarnold, Sutton:** Tumour RT fraction size sensitivity; how variable is it?
14.05	**Rob Bristow, Toronto:** Predicting radiotherapy outcome using somatic genetics in prostate cancer
14.25	**Jan Alsner, Aarhus:** Genetic variants and normal tissue toxicity after radiotherapy
14.45	Discussion
15.00-15.20	Coffee break
15.20-17.00	**Session 2: Pre-clinical biological imaging of tumours** Chairpersons: M. Nordsmark and E. Malinen
	Keynote lectures
15.20	**Vincent Gregoire, Brussels:** The use of functional imaging for radiotherapy planning: "plug and play" or how much validation do we need?
15.40	**Andreas Kjær, Copenhagen:** Molecular imaging with PET for tailored cancer therapy
16.00	**Michael Horsman / Thomas Nielsen, Aarhus:** Nano-based MR-approaches for imaging the tumour vasculature and microenvironment
	Proffered papers
16.20	**Kathrine Røe, Oslo:** Kinetic analysis of dynamic 18F-FDG PET imaging of prostate carcinoma xenografts – tumorbiological characterization and radiation response evaluation

(cont...)

16.30	**Morten Busk, Aarhus:** Hypoxia PET imaging: defining the added value of dynamic scan protocols
16.40	**Åste Søvik, Oslo:** Adaptive radiotherapy based on contrast enhanced cone beam CT imaging
16.50	Discussion
17.00-18.00	**Poster viewing bar**
19.00	**Welcome reception – AROS Art Museum, City Center** Guided tours start at 19.15 Dinner 20.00

Please remember your entrance ticket

Thursday May 27, 2010

8.20 - 10.20	**Session 3: Functional imaging and treatment planning** Chairpersons: K. Tanderup and V. Gregoire
8.20	**Vincent Gregoire, Brussels:** Introduction
	Keynote lectures
8.30	**Uulke van der Heide, Utrecht:** Functional imaging of prostate: from radiology to radiotherapy
8.50	**Anca-Ligia Grosu, Heidelberg:** PET for GTV delineation in brain tumors
9.10	**Stine Korreman, Madison:** Feasibility and robustness of dose painting by numbers using arc therapy techniques
	Proffered papers
9.30	**Søren Haack, Aarhus**: Distribution of low diffusion regions as observed with diffusion weighted MRI in relation to GEC ESTRO targets used for brachytherapy in locally advanced cervical cancer
9.40	**Indira Madani, Ghent:** Adaptive dose painting by numbers for head and neck cancer
9.50	**Fredéric Duprez, Ghent:** A phase I clinical trial on adaptive dose painting by numbers for head and neck cancer: the first clinical results
10.00	**Anne K. Due, Copenhagen:** Methodologies for localizing head and neck cancer recurrences in relation to radiation therapy target volumes
10.10	Discussion
10.20 - 10.50	Coffee break and poster viewing
10.50 - 12.00	**Session 4: Imaging of normal tissue function** Chairpersons: M. Høyer and J. Deasy
	Keynote lectures
10.50	**Yue Cao, Ann Arbor:** Functional imaging as a biomarker for radiation-induced normal tissue and organ toxicity
11.10	**Mike Partridge, Sutton:** Functional imaging of normal lung in radiotherapy
11.30	**Morten Høyer, Aarhus:** Functional imaging of liver for radiotherapy
11.50	Discussion
12.00 - 13.00	Lunch

13.00 - 14.10 **Session 5: Functional imaging segmentation, registration and quantification**
Chairpersons: J. Lindegaard and U. van der Heide

Keynote lectures

13.00 **Marc Kessler, Ann Arbor:** Tools of our trade: segmentation and registration for planning, delivery and adaptation

13.20 **Robert Jeraj, Madison:** How much can we trust images for Biology-guided Adaptive Radiotherapy?

Proffered papers

13.40 **Thea Sollien, Oslo:** Histogram analysis of pharmacokinetic parameters derived from dynamic contrast enhanced imaging

13.50 **Erlend Andersen, Oslo:** Histogram-based segmentation of regions at risk in cervical cancers by dynamic contrast enhanced MRI and pharmacokinetic modelling

14.00 Discussion

14.10 - 14.40 Coffee break
Poster viewing

14.40 - 16.40 **Session 6: Quantitative analysis and modelling of clinical outcome**
Chair: L. P. Muren and M. Partridge

Keynote lectures

14.40 **Philippe Lambin, Maastricht**: Voxel control / complication probability

15.00 **Eirik Malinen, Oslo:** TCP modelling of biological image guided radiotherapy

15.20 **Joseph Deasy, St. Louis:** Are current NTCP models reliable guides for treatment plan optimization?

Proffered papers

15.40 **Iuliana Toma-Dasu, Stockholm:** Dose painting by numbers - are the practical limitations of the technique decreasing or increasing the probability of controlling the tumour?

15.50 **Pauliina Wright, Oslo/Aarhus:** Evaluation of adaptive radiotherapy of bladder cancer using image-based tumour control probability modelling

16.00 **Ivan Vogelius, Madison:** Risk of radiation pneumonitis is insensitive to hypofractionation with modern conformal radiation delivery techniques

(cont..)

16.10 **Tine Schytte, Odense:** Mean radiation dose to the heart and risk of cardiac toxicity in NSCLC treated with definitive radiotherapy

16.20 **Maria Thor, Aarhus:** Rectum motion and morbidity prediction: improved correlation between late morbidity and DVH parameters for rectum planning organ at risk volumes

16.30 Discussion

16.40 - 17.30 **Poster viewing bar**

19.00 **Conference dinner – Varna Mansion (next to Hotel Marselis)**

Friday May 28, 2010

8.20 - 10.10 **Session 7: Adaptive strategies and technologies**
Chairpersons: C. Grau and M. Kessler

Keynote lectures

8.20 **Karin Haustermans, Leuven:** How to adapt the multimodal treatment in rectal cancer based on imaging?

8.40 **Richard Pötter, Vienna:** Is repetitive morphologic imaging valuable for Bigart?- Experience from MRI based adaptive cervix brachytherapy (GynART).

9.00 **Martin Fuss, Portland:** Strategies of assessing and quantifying post-treatment metabolic tumor response

Proffered papers

9.20 **Anne Vestergaard, Aarhus:** Adaptive strategies for radiotherapy of bladder cancer – a feasibility study

9.30 **Marianne Knap, Aarhus:** Daily cone-beam computed tomography used to determine tumour shrinkage in lung cancer patients

9.40 **Sune K. Buhl, Herlev**: Clinical evaluation of 3D/3D MRI-CBCT automatching on brain tumors for online patient setup verification – A step towards MRI-based planning

9.50 **Per R. Poulsen, Aarhus:** DMLC tracking of moving targets with a single kV imager for static field treatments

10.00 Discussion

10.10 - 10.30 Coffee break

10.30 - 11.40 **Session 8: Particle therapy**
Chairpersons: D. R. Olsen and R. Pötter

Keynote lectures

10.30 **Håkan Nyström, Uppsala:** The role of protons in biologically guided adaptive radiotherapy

10.50 **Stephanie Combs, Heidelberg:** Heidelberg Ion Therapy Center - Experience with the first 100 patients

(cont…)

	Proffered papers
11.10	**Per Munck af Rosenschöld, Copenhagen:** On-line adaptive intensity modulated proton therapy of lung cancer – a treatment planning study of 2D tracking
11.20	**Niels Bassler, Aarhus:** Dose- and LET-painting with particle therapy
11.30	Discussion
11.40 - 12.00	**Session 9: Conference wrap-up** Chairperson: L.P. Muren
	Keynote lecture
11.40	**Dag Rune Olsen, Bergen:** BiGART2010, impressions and future aspects
12.00	Closing of the meeting

The symposium is generously supported by:

ACTA ONCOLOGICA

CIRRO The Lundbeck Foundation Center for Interventional Research in Radiation Oncology

Posters

on display throughout the meeting

1. Daily KV cone-beam CT and deformable image registration as a method for studying dosimetric consequences of anatomic changes in adaptive IMRT of head and neck. Ulrik Vindelev Elstrøm, Aarhus, Denmark

2. Investigation of respiration induced intra- and inter-fractional tumour motion using a standard Elekta Cone Beam CT. Karina Lindberg Gottlieb, Odense, Denmark

3. A novel mathematical model for the radiobiological evaluation of an adaptive course of treatment. Francisco Cutanda Henríquez, Madrid, Spain

4. Investigation of the dosimetric impact of a Ni-Ti fiducial marker in carbon and proton beam. Rochus Herrmann, Aarhus, Denmark

5. Neutron fluence in antiproton radiotherapy measurements and simulations. Niels Bassler, Michael Holzscheiter, Heidelberg, Germany

6. ConeBeam CT for setup of patients with cancer in the cervix uterus: Comparing 3D match with 6D match on the whole body as well as soft tissue. Kirsen Legård Jakobsen, Herlev, Denmark

7. Feasibility and Sensitivity Study of Helical Tomotherapy for Dose Painting Plans. Robert Jeraj, Madison, USA

8. Uncertainty of textural features in PET images due to different acquisition mode and reconstruction parameters. Robert Jeraj, Madison, USA

9. Robustness of Apparent diffusion coefficient (ADC) diffusion weighted MR imaging in cervical cancer. Dependence on B-values used. Jesper Folsted Kallehauge, Aarhus, Denmark

10. Adaptive field margin: Accounting for interfraction motion variation offers negligible effect for most patients. Stine Korreman, Copenhagen, Denmark

11. Investigation of breast Setup accuracy using both surgical clips and patient anatomy with the Exactrac ® and 2D/3D on-board imager ® systems. Brian Kristensen, Herlev, Denmark

12. Changes in target delineation for high grade glioma using 18 FDG PET fused with MRI and CT. Yasmin Alexandra Lassen, Aarhus, Denmark

13. Residual rotational set-up errors after daily cone-beam CT image guidance in locally advanced cervical cancer. Louise Vagner Laursen, Aarhus, Denmark

14. Identifying hypoxia in human tumors: a correlation study between FMISO PET and the Eppendorf oxygen electrode. Lise Saksø Mortensen, Aarhus, Denmark

15. Non-invasive imaging of combretastatin activity in different tumour models: association with more invasive estimates. Thomas Nielsen, Aarhus, Denmark

16. Influence of the fixation and imaging protocol on the treatment margin for thoracic patients – a multi centre study. Tine Bjørn Nielsen, Odense, Denmark

17. IGRT in squamous cell carcinoma esophageal cancer – experiences with cone beam CT. Marianne Nordsmark, Aarhus, Denmark

18. Single institution experience from 100 patients included in Danish Breast Cancer Cooperative Group (DBCG) radiation protocols: compromise is necessary between dose to the left anterior descending coronary artery and breast clinical target volume. Birgitte Offersen, Aarhus, Denmark

19. On the potential use of alanine for small field output factor determination in high energy photon beams – a Monte Carlo study. Rickard Ottosson, Herlev, Denmark

20. Evaluation of NSCLC patient setup accuracy by investigating 3 and 6 degrees-of-freedom CBCT auto matches, based on whole thorax, columna vertebralis and GTV. Wiviann Ottosson, Herlev, Denmark

21. Influence of MLC leaf width on biologically adapted IMRT plans. Jan Rødal, Oslo, Norway

22. Comparison of manual and automatic segmentation for FDG PET based tumor delineation in head and neck cancer. Hella M.B. Sand, Aalborg, Denmark

23. Dose calculation in biological samples in a mixed neutron-gamma-field at the University of Mainz. Tobias Schmitz, Mainz, Germany

24. A phantom treatment planning study of the distribution of dose-averaged LET in small volumes irradiated with ^{12}C. Christian Skou Søndergaard, Aarhus, Denmark

25. A study of image-guided radiotherapy of bladder cancer based on lipiodol injection in the bladder wall. Jimmi Søndergaard, Aarhus, Denmark

26. Identifying pH independent hypoxia induced genes in human squamous cell carcinomas in vitro. Brita Singers Sørensen, Jan Alsner, Aarhus, Denmark

27. Propagation of target and organ at risk contours in prostate radiotherapy using deformable image registration. Sara Thörnqvist, Aarhus, Denmark

28. Stereotactic body radiotherapy: Relationship of setup errors to body mass index and treatment time. Esben Schjødt Worm, Aarhus, Denmark

NACP
Nordic Association for Clinical Physics

ACTA ONCOLOGICA

ACTA Oncologica Symposium on Particle Therapy
&
NACP 2011 Symposium

A dual event addressing particle therapy and multidiciplinary nordic cooperation in medical physics

www.nacp-nordisk.org

Uppsala, 13-15 April 2011
Norrlands Nation
Uppsala, Sweden

Swedish Society for Radiation Physics

AKADEMISKA SJUKHUSET

SSFF
Swedish hospital physicists association

Wednesday May 26, 2010

Session 1: Radiobiology

John Yarnold, Sutton, UK

Radiotherapy fraction size sensitivity in breast cancer

John Yarnold. *Section of Radiotherapy. Institute of Cancer Research & Royal Marsden Hospital Sutton, UK.*

The results of 5 published randomised trials testing hypofractionation in >7,000 women prescribed adjuvant post-operative radiotherapy for early breast cancer are consistent with the hypothesis that breast cancer has a similar sensitivity to fraction size as the dose-limiting late reacting normal tissues. A metanalysis of the START pilot and START A trials generated a direct estimate of α/β of 4.6 Gy (95%CI 1.1-8.1) for local tumour control, based on 294 events in 3646 patients [1-2]. Although the average fractionation sensitivity is comparable with that of late reacting normal tissues, fractionation sensitivity is likely to vary from one tumour to another, and subgroups may exist that differ in their responses to hypofractionation. Predictive biomarkers of fractionation sensitivity would help individualise selection of fraction size.
Sensitivity to fraction size has long been understood to have a basis in the process of cellular recovery, and is not a fixed parameter. For example, if radiotherapy treatment time is <14 days, acute human epidermal responses are more sensitive to fraction size (α/β value ~ 4 Gy) than if radiotherapy is delivered over longer periods (α/β values > 10 Gy) [3]. A clue to the difference lies in changes in the proliferation kinetics of basal epidermis during fractionated radiotherapy. The fall in epidermal fractionation sensitivity is associated over a 5-week course of treatment with an increase in proliferative indices in the basal epidermis. Squamous carcinomas tend to have high proliferative indices and display low fraction size sensitivity (high α/β values) relative to breast and prostate cancers. A molecular model of clinical fractionation sensitivity is based on the predominance of NHEJ (postulated to be sensitive to fraction size) in slowly proliferating tissues and the predominance of HR (postulated to be insensitive to fraction size) in rapidly proliferating tissues. The aim of our current research is to test the hypothesis that fractionation sensitivity is associated with proliferation status of the tumour and with the DNA repair mechanism used to repair DSB. One approach tests for association between tumour Ki67 index of relapsed and non-relapsed breast cancers treated with different randomly allocated fractionation schedules. The long-term aim is to identify predictive bio-markers of fractionation sensitivity that help to individualise radiotherapy regimen in breast cancer and other tumour types.

[1] Owen JR, Ashton A, Bliss JM, et al. Effect of radiotherapy fraction size on tumour control in patients with early-stage breast cancer after local tumour excision: long-term results of a randomised trial. Lancet Oncol 2006;7:467-471.

[2] Bentzen SM, Agrawal RK, Aird EG, et al. The UK Standardisation of Breast Radiotherapy (START) Trial A of radiotherapy hypofractionation for treatment of early breast cancer: a randomised trial. Lancet Oncol 2008;9:331-341.

[3] Hopewell JW, Nyman J Turesson I. Time factor for acute tissue reactions following fractionated irradiation: a balance between repopulation and enhanced radiosensitivity. Int J Radiat Biol 2003;79:513-524.

Wednesday May 26, 2010

Robert Bristow, Toronto, Canada

DNA Copy Number Alterations and Prediction Of Biochemical Recurrence Following Radiotherapy In Intermediate Risk Prostate Cancer

Robert Bristow MD PhD FRCPC. *Departments of Radiation Oncology and Medical Biophysics, and Laboratory Medicine and Pathology, University of Toronto and Ontario Cancer Institute/ Princess Margaret Hospital-University Health Network, Toronto, ON, Canada.*

Prostate cancer is the most common cancer in man with more than 250,000 men being diagnosed in North America. Greater than 30,000 of these men will die of the disease. Current prognostic variables including T-category (of the TNM staging), the absolute or kinetics of Prostatic Specific Antigen (PSA) and the pathologic Gleason Score (GS) are utilized to place men in low, intermediate and high-risk prostate cancer risk groupings. These risk groupings determine the risk for not only local control following therapy but also systemic metastases. As such, specific treatments and management is driven by the use of these clinical prognostic groupings in the overall management of prostate cancer. Despite this, there is still great heterogeneity in biochemical recurrence in this risk group. Our aim was to identify genomic copy number alterations (CNA's) that are independently associated with biochemical failure following image-guided radiotherapy (IGRT).

High-resolution array comparative genomic hybridization (aCGH) was performed on needle biopsies derived from 115 intermediate risk patients prior to IGRT to the prostate gland alone. IGRT doses were 70-80 Gy (2 Gy/day) in 101 patients and 60-66Gy (3 Gy/day) in 14 patients. Neoadjuvant and concurrent hormonal therapy (bicalutamide 150 mg od) was used in 25 patients. Clinical covariates were T category (36 T1c, 78 T2), Gleason score (1 G5, 30 G6, 84 G7) and pretreatment PSA (range 0.93-18.78 ng/ml). Median follow-up was 5.2 years. The outcome variable was time to biochemical failure (BF), defined by the Phoenix criteria or the initiation of salvage therapy. 22 regions with CNA loss or gain were observed in greater than 20% of patients and each was tested for its association with BF using a logrank test. The percentage failure free was calculated and plotted using the Kaplan-Meier approach. Associations between the clinical factors and all CNA regions were investigated using the Fisher exact test.

aCGH identified significant variation in CNA within this homogenous clinical risk group with the percentage of genome altered (PGA) ranging from < 1% to 35%. BF was observed in 33/115 patients. On multivariate analysis controlling for the clinical covariates, PGA predicted for BF with higher statistical significance than either T-category or Gleason score (p=.00016). Further, 3 CNA regions were independently associated with poorer DFS: (p = 0.01-04). Associations between these regions, PTEN loss, c-MYC amplification and p53 mutation along with clinico-pathologic data will be presented.

This is the largest reported study of CNA's in intermediate risk prostate cancer. Global PGA (a surrogate for tumor genetic instability), and three specific genomic alterations, are independently associated with biochemical recurrence after IGRT. Current work includes associating specific genes to these prognostic CNA's to develop a genetic signature capable of predicting individualized radiotherapy response. Supported by the Terry Fox Foundation, Canadian Cancer Society Research Institute, Prostate Cancer Canada and the Ontario Institute for Cancer Research. RGB is a Canadian Cancer Society Research Scientist.

Wednesday May 26, 2010

Genetic variants and normal tissue toxicity after radiotherapy

Jan Alsner. *Department of Experimental Clinical Oncology, Aarhus University Hospital, Denmark.*

During the last decade, a number of studies have supported the hypothesis that there is an important genetic component to the observed interpatient variability in normal tissue toxicity after radiotherapy. Genetic markers with sufficient predictive power to be used at an individual level have not been identified yet. Although it is still an open question whether such markers can be identified, some progress has been made recently, particularly, for predicting late toxicity. Some of the more promising predictive assays are based on lymphocytes or fibroblasts. Commonly following in vitro irradiation, gene expression profiles are measured or functional assays are recorded and used to identify individuals with low or high risk of normal tissue toxicity. Although the technical set-up for these assays makes it unlikely that they will enter any routine clinical settings, they allow the identification of genes that are involved in the development of radiation induced morbidity. These genes, or the pathways in which they are functioning, could be relevant targets for intervention and might also lead to the identification of candidate genes for single nucleotide polymorphism (SNP) association studies. So far, most of the SNP association studies reported have been limited by the inclusion of low numbers of patients with different kinds of normal tissue toxicity. Future genetic association studies will be equally impeded by the difficulties in characterising well-defined clinical and biological phenotypes and handling of the many confounding factors.
Recently, an International Radiogenomics Consortium has been established. The primary aim of the consortium is to develop an assay capable of predicting which cancer patients are most likely to develop radiation injuries resulting from treatment with a standard radiotherapy protocol. A second aim is to obtain information to assist with the elucidation of the molecular pathways responsible for radiation-induced normal tissue toxicities through identification of genes possessing SNPs associated with the development of radiation-induced adverse effects. The rationale underlying the consortium is that the international scientific community must work together to provide definitive answers regarding the importance of individual SNPs through the performance of adequately powered studies which require many thousands of patients. The consortium provides a forum for sharing best practice in terms of collecting toxicity and confounding variable data (particularly dose volume histogram data), in genotyping and for the analysis of genetic associations with toxicity.

Session 2: Pre-clinical biological imaging of tumours

Vincent Gregoire, Brussels, Belgium

The use of functional imaging for radiotherapy planning: "plug and play" or how much validation do we need?

Vincent Gregoire. *Radiation Oncology Dept. and Center for Molecular Imaging and Experimental Radiotherapy, Université Catholique de Louvain, Brussels, Belgium.*

Biological image-guided radiotherapy aims at specifically irradiating biologically relevant subvolumes within the tumor, as determined for instance by PET imaging. This approach requires that PET imaging be sensitive and specific enough to image various biological pathways of interest, e.g. tumor metabolism, proliferation and hypoxia. In this framework, the use of PET imaging for adaptive radiotherapy needs to be evaluated in term of accuracy and added value in comparison with standard procedures.
It first requires the optimization of the PET image quality during the acquisition and the reconstruction, to try to improve the spatial resolution, the level of noise and the contrast, that are typical features of PET imaging. Thereafter, it requires robust and validated tools for accurate segmentation of the regions of interest. The blur effect related to the poor spatial resolution of the camera and the high level of noise severely corrupt the images, and consequently interfere with the tumor segmentation. The use of “image restoration tools” for deblurring and denoising PET images before any segmentation represents an elegant way to improve image quality. Associated with a gradient-based segmentation technique, this approach has been shown to outperform the conventional threshold-based methods. However, even when using optimal procedures for image acquisition, reconstruction and segmentation, one has to keep in mind that there will always exist some discrepancies between the information from a PET image and the underlying microscopic reality. Such differences may be of critical importance when considering giving boost doses to small and highly active PET regions. This issue should be carefully looked at before applying on a clinical routine basis sub-volume segmentation with some form of dose-painting. Last outcome studies should be ideally performed as an ultimate endpoint to ascertain the clinical benefit of the use of functional imaging in routine practice.

Wednesday May 26, 2010

Andreas Kjær, Copenhagen, Denmark

Molecular Imaging with PET for Tailored Cancer Therapy.

Andreas Kjær. *Cluster for Molecular Imaging & Dept. of Clinical Physiology, Nuclear Medicine & PET, Rigshospitalet, University of Copenhagen, Denmark.*

The movement in direction of individualized, tailored cancer therapy has led to a need for diagnosing at the molecular level. In contrast to currently used molecular biology methods that rely on tissue sampling for in vitro diagnostics, molecular imaging allows for non-invasive studies at the molecular level in intact organisms. With positron emission tomography (PET) and specific tracers it is possible to visualize tissue characteristics of importance for how cancer patients should be treated. Examples will be given illustrating how such PET scans may be used for selection of patients suited for therapies as well as for planning, dosing and monitoring of anti-cancer treatment.

With PET we can study hypoxia leading to therapy resistance, angiogenesis that may be inhibited by specific drugs and cell proliferation and programmed cell death (apoptosis) that allows for detection of treatment response already after few hours. Finally, we may visualize the invasive phenotype and predict how fast the cancer will spread.

The use of these molecular imaging methods will lead to more effective and gentle treatment of cancer patients in the future.

Wednesday May 26, 2010

Kathrine Røe, Oslo, Norway

Kinetic analysis of dynamic ^{18}F-FDG PET imaging of prostate carcinoma xenografts – tumorbiological characterization and radiation response evaluation

[1,2]Røe K, [2]Aleksandersen TB, [1]Kristian A, [1,2]Nilsen LB, [1]Seierstad T, [2]Qu H, [1,2]Ree AH, [3]Olsen DR, [2,4]Malinen E. *[1]Institute for Cancer Research, Oslo University Hospital, Oslo, Norway, [2]University of Oslo, Oslo, Norway, [3]University of Bergen, Bergen, Norway, [4]Department of Medical Physics, Oslo University Hospital, Oslo, Norway.*

Introduction: Individualized cancer medicine requires reliable, non-invasive tumor visualization of underlying vascular, molecular and physiological mechanisms of importance in prognosis and treatment response. The purpose of this study was to establish a dependable analysis tool for extraction of kinetic parameters from dynamic PET (dPET) acquisitions, and to assess the feasibility of this model in radiation response monitoring.

Materials and methods: Male, athymic mice with s.c. prostate carcinoma xenografts were subjected to dPET either untreated (n = 6) or 24 h post-radiation (7.5 Gy single dose, n = 7). After 10 h of fastening, i.v. bolus injections of 10 – 15 MBq ^{18}F-FDG were administered and a 1 h dPET scan was performed (microPET Focus 120, Siemens, Germany). Attenuation correction was obtained by a 10 min scan with a ^{68}Ge point source. 3D dynamic emission data were reconstructed using OSEM-MAP, before post-processing in IDL (v6.2, Boulder, CO). Individual arterial input functions and tumor delineations were extracted and subjected to voxel-by-voxel two-tissue compartment modeling to produce kinetic, tumorbiological maps.

Results: The model separated the ^{18}F-FDG uptake into unbound and bound (metabolized) tracer and quantified three parameters; forward (k_1) and backward (k_2) tracer diffusion, and rate of ^{18}F-FDG phosphorylation, or glucose metabolism (k_3). The kinetic model demonstrated a goodness of fit (r^2) to the observed data ranging from 0.93 to 0.98, and produced parametrical images of all tumors included in the study. Untreated tumors showed similar values of k_1, k_2 and k_3, whereas the parameters significantly increased in the tumors exposed to a 7.5 Gy radiation dose 24 h before ^{18}F-FDG PET.

Conclusions: The study demonstrates the feasibility of a two-compartment kinetic analysis of dynamic ^{18}F-FDG PET images. Extracted parametrical maps may be used in tumor characterization, radiation response monitoring and facilitation of tumor delineation.

Wednesday May 26, 2010

Morten Busk, Aarhus, Denmark

Hypoxia PET imaging: Defining the added value of dynamic scan protocols

Busk M[1], Horsman MR[1], Jakobsen S[2], Hansen KV[2], Bussink J[3], van der Kogel A[3] and Overgaard J[1]. *1) Department of Experimental Clinical Oncology, Aarhus University Hospital (AUH), Aarhus, Denmark. 2) PET centre, AUH. 3) Department of Radiation Oncology, Radboud University Nijmegen Medical Centre, Nijmegen,The Netherlands.*

Introduction: PET allows detection and mapping of tumor hypoxia. However, slow tracer retention, slow clearance of unbound tracer and low resolution, results in limited image contrast and the risk of missing areas where hypoxic cells and necrosis are intermixed, even on late-time static scans. It has been proposed that the shape of time activity curves (TACs) deduced form dynamic scans, allows further, clinically useful, separation of tumors or individual voxels that are inseparable based on static scans. This study was designed to clarify the added value of dynamic scans.

Materials: Human or murine squamous cell carcinomas were grown in mice. Mice were injected with the PET hypoxia-tracer fluoroazomycin arabinoside (FAZA) and the proven immunologically-detectable hypoxia-marker, pimonidazole and scanned dynamically for up to 6h, followed by tissue sampling. Tumor sections were analysed for microregional tracer retention (autoradiography), distribution of pimonidazole-retaining hypoxic cells (immunofluorescence) and necrosis.

Results/Discussion: All tumor models retained FAZA relative to reference tissue at late time points. The post-scan deduced microregional distribution of FAZA (autoradiograms) and hypoxic cells (pimonidazole-adduct fluorescence) was in excellent agreement and revealed that most tumors contained hypoxic areas. TACs shapes, however, varied widely ranging from distinctly wash-out to accumulative types, and the overall shape was largely tumor-type dependent rather than determined by the actual extent of hypoxia, suggesting that the interpretation of TAC shapes is challenging. More detailed kinetic analysis of dynamic scans is ongoing and will clarify whether any significant gain in accuracy is added by using a clinically less attractive dynamic scan protocol.

This study was supported by EC FP6 and FP7 funding, by CIRRO - The Lundbeck Foundation Center for Interventional Research in Radiation Oncology, and The Danish Council for Strategic Research.

Wednesday May 26, 2010

Åste Søvik, Oslo, Norway

Adaptive radiotherapy based on contrast enhanced cone beam CT imaging

Søvik Å[1,2], Rødal J[2], Skogmo HK[1], Lervåg C[2], Eilertsen K[2], Malinen E[2]. *[1]Department of Companion Animal Clinical Sciences, Norwegian School of Veterinary Science, Oslo, Norway, [2]Department of Medical Physics, The Norwegian Radium Hospital, Oslo University Hospital, Oslo, Norway.*

Introduction: Cone beam CT (CBCT) imaging has become an integral part of radiation therapy, with images typically used for offline or online patient setup corrections based on bony anatomy coregistration. Ideally, the coregistration should be based on tumor localization. However, soft tissue contrast in CBCT images is limited. In the present work, contrast enhanced CBCT (CECBCT) images were used for tumor visualization and treatment adaptation.

Materials and Methods: A spontaneous canine maxillary tumor was subjected to repeated cone beam CT imaging during fractionated radiotherapy (10 fractions in total). At five of the treatment fractions, CECBCT images were acquired, as well as pre-contrast CBCT images. The tumor was clearly visible in post-contrast minus pre-contrast subtraction images, and these contrast images were used to delineate gross tumor volumes. IMRT dose plans were subsequently generated. Three different adaptive strategies were explored: 1) replanning based on each CECBCT image series, 2) planning based on images acquired at the first treatment fraction and patient repositioning following bony anatomy coregistration, 3) as for 2), but with patient repositioning based on coregistering contrast images. These adaptive strategies were compared to a strategy with no patient repositioning or treatment adaptation, using equivalent uniform dose (EUD) and tumor control probability (TCP) calculations to estimate treatment outcome.

Results: Similar translation vectors were found when bony anatomy and contrast enhancement coregistration were compared. Strategy 1 gave EUDs closest to the prescription dose and the highest TCP. Strategies 2 and 3 gave EUDs and TCPs close to that of strategy 1, with strategy 3 being slightly better than strategy 2. Even greater benefits from strategies 1 and 3 are expected with increasing tumor movement or deformation during treatment. The non-adaptive strategy was clearly inferior to all three adaptive strategies.

Conclusion: CECBCT may prove useful for adaptive radiotherapy.

Thursday May 27, 2010

Session 3: Functional imaging and treatment planning

Uulke van der Heide, Utrecht, The Netherlands

Functional imaging of prostate: from radiology to radiotherapy

Van der Heide, U.A., Groenendaal G., Korporaal, J.G., Van Vulpen, M. *Department of Radiotherapy, University Medical Center Utrecht, Utrecht, The Netherlands.*

Introduction: Dynamic Contrast-Enhanced (DCE) MRI and Diffusion-weighted MRI (DWI) are frequently used for the diagnosis of prostate cancer. A high tissue perfusion and a low diffusion of water are associated with the presence of tumor. Application for target delineation in radiotherapy raises some specific issues. At what spatial resolution can these techniques be used reliably? And do the two techniques identify the same regions as suspicious, or do they provide complementary information?

Materials and methods: Patients scheduled for prostate radiotherapy, routinely received a 3T MRI exam, including a T2-weighted scan, DCE-MRI and DWI. DCE-MRI data were analyzed using the Tofts model, yielding 3D maps of the blood flow parameter Ktrans. From the DWI scans Apparent Diffusion Coefficients (ADC) were calculated. The parameter maps were compared using a receiver operating curve (ROC) analysis, where either one of the two imaging modalities was thresholded and taken as a reference. The resulting area under the curve (AUC) reflects the consistency between target delineations based on the two imaging techniques. The repeatability of Dynamic contrast-enhanced imaging was tested on CT. 29 patients received two DCE-CT exams within one week. Analysis with the Tofts model was done at 15 different image resolutions. The voxelwise repeatability was determined using a Bland-Altman analysis.

Results: The consistency between DWI and DCE-MRI parameter maps varied substantially between patients, with AUC values in the peripheral zone ranging from 0.44 to 0.9. The repeatability of DCE-CT was high at voxels as small as 0.15 cc.

Conclusion: While DCE imaging techniques are sufficiently repeatable for delineation of prostate tumors, differences emerge between the volume identified as suspect on DCE-MRI and DWI. A pragmatic approach is required to deal with these inconsistencies in clinical practice, while further research is needed to understand the origin of this difference.

Thursday May 27, 2010

Anca-Ligia Grosu, Freiburg, Germany

PET for GTV Delineation in Brain Tumors

Anca-Ligia Grosu, *Department for Radiation Oncology, University of Freiburg, Germany*

In brain tumors, the planning of the treatment and the evaluation of the local response to therapy are usually based on magnetic resonance imaging (MRI) and computed tomography (CT). These investigations show the anatomy of the brain with a high accuracy. However, contrast enhancement or hyperintensity on T2- or flair-MRI are not tumor specific. Tumor tissue can be located also in the iso-intense areas. Moreover, after surgery, radiation, chemotherapy etc. treatment-related changes, like blood-brain-barrier (BBB) disturbance or edema, generally cannot be differentiated from viable tumor tissue. New concepts like pseudo-progression or pseudo-remission were introduced (for brain gliomas) to describe the fact that the morphological imaging is insufficient for the visualization of tumor tissue after therapy. New MRI methods like diffusion and perfusion MRI or MRI spectroscopy are promising investigation techniques. However, there are not enough data in the literature defining the sensitivity and the specificity of these investigations based on histological results. Hence, it is early to speak about the integration of diffusion or perfusion MRI in radiation treatment planning. MRI spectroscopy has a long tradition. Unfortunately, the method remains relatively laborious and has a low resolution. Therefore, there is an urgent need for new imaging approaches to increase tumor delineation for high precision radiotherapy.

Imaging the biological and molecular characteristics of the tumor tissue by PET is an interesting approach to improve treatment planning for high precision radiotherapy. In the first part of this chapter we will discuss the role of AA-PET for gross tumor volume (GTV) delineation in brain gliomas, metastases and benign cranial tumors like meningiomas and glomus tumors. In the second part we will focus our attention on tracers used to visualize biological properties of the tumors like hypoxia, proliferation or expression of peptide/protein on the cell membrane.
^{11}C-labeled methionine (MET), ^{123}I-labeled alpha-methyl-tyrosine (IMT) and ^{18}F-labeled O-(2) fluoroethyl-L-tyrosine (FET) are the most important radio-labeled amino acids used in the diagnosis of brain tumors. These three tracers have shown a very similar uptake intensity and distribution in brain tumor. Currently available amino acid PET tracers are accumulated by L and A amino acid transporters. Tumor cells take up radio-labeled amino acids at a high rate, while there is only a relatively low uptake in normal cerebral tissue. At the level of the blood-brain barrier (BBB) they are independent from the BBB disturbance.

The higher sensitivity and specificity of AA-PET in the diagnosis of gliomas in comparison to CT and MRI was demonstrated in many clinical trials. Summarizing the data of the literature we found between 1983 and 2007 45 trials including 1721 patients, which investigated the role of MET-PET in diagnosis of gliomas. Eleven studies including 706 patients were based on PET/MRI/CT stereotactical biopsies. Between 2000 and 2007 12 trials including 361 patients evaluated the role of FET-PET in the diagnosis of brain gliomas. In 3 studies evaluating 126 pa-

tients the results were based on PET/MRI/CT stereotactic biopsies. All these studies have shown that the specificity of MET-PET and FET-PET for malignant gliomas is significantly higher (85-95%) in comparison to MRI, which has a high sensitivity but a lower specificity (ca. 50%).

The similarity between MET- and FET-PET for tumor visualization was demonstrated in many studies. We investigated 42 patients with gliomas and metastases in the same day on MET- and FET-PET. We found an almost identical sensitivity and specificity of the both tracers. Furthermore, the intensity of tracer uptake and the extension of gliomas in FET-PET were closely correlated with the extension in MET-PET. Thus, these studies indicate that the results of MET-PET can be extrapolated to FET-PET and that MET-PET and FET-PET can be used in this trial.

The higher diagnostic accuracy of AA-PET is the rationale for using this technique in target volume delineation of gliomas, since AA-PET can also provide information regarding tumor extension. In a series of clinical studies we demonstrated marked differences between AA-PET or SPECT and MRI in GTV delineation for radiation treatment planning. In 39 patients with high grade gliomas imaged postoperatively tumor contrast enhancement in MRI and AA uptake corresponded in only 13% of the patients. On average 13 ml (33%) of the tumor volume defined on AA-PET demonstrated no contrast enhancement on MRI.

Based on these data we performed a small prospective single center study, in which AA-PET or AA-SPECT was used for planning of stereotactic radiotherapy. In this study patients with recurrent gliomas lived significantly longer when AA-PET or single photon emission tomography (AA-SPECT) were integrated in target volume delineation. Median survival of patients who underwent AA-PET or -SPECT based radiation treatment was 4.5 months longer than of patients who underwent CT/MRI based radiation treatment. This was the first study indicating that radiation therapy guided by AA-PET can improve patient survival. A randomized trial is planed, having the aim to confirm (or infirm) this exciting observation in a multicenter setting.

Thursday May 27, 2010

Stine Korreman, Madison, USA

Feasibility and robustness of dose painting by numbers using a volumetric modulated arc therapy technique

Korreman S (1,2,3), Ulrich S (1), Bowen S (4), Deveau M (4), Bentzen SM (2), Jeraj R (2,4). *1) Department of Radiation Oncology, Rigshospitalet, Copenhagen, Denmark. 2) Department of Human Oncology, University of Wisconsin, Madison, USA. 3) Niels Bohr Institute, University of Copenhagen, Copenhagen, Denmark. 4) Department of Medical Physics, University of Wisconsin, Madison, USA.*

Purpose: Dose painting strategies are limited in practice by the optimization algorithms in treatment planning systems and the physical constraints of the beam delivery. This study aims to investigate dose conformity for dose painting using the RapidArc optimizer and beam delivery technique. Furthermore, robustness of the plans with respect to positioning uncertainties are evaluated.

Methods: A head & neck cancer patient underwent a [^{61}Cu]Cu-ATSM PET/CT scan. PET SUVs were converted to prescribed doses with a base dose of 60Gy (in 2Gy fractions), and overall target mean dose of 90Gy. The voxel-based prescription was subsequently converted into five discrete prescription levels. Optimization was performed using the Eclipse inverse arc optimizer, varying the following parameters: MLC leaf width (5 mm and 2.5 mm), number of arcs (1 and 2) and collimator rotation (0, 15, 30 and 45 degrees). Dose conformity was evaluated using quality volume histograms (QVHs) normalised to the discretized dose levels, and magnitudes of relative volumes receiving within ±5% of the prescribed dose ($Q_{0.95–1.05}$). Deliverability was tested for a subset of plans using a Delta4 phantom, and consistency was quantified using gamma analysis (3%-1mm criteria). Robustness was tested by shifting the isocenter of the plans (simulating systematic positional error) by 1mm and 2mm in all directions, and recalculating the planned dose.

Results: Good conformity was obtained using the MLC with 2.5 mm leaf width, two arcs, and collimators in 45/315 degrees, with $Q_{0.95–1.05}$=79.2% . Using only one arc or increasing the MLC leaf width had a small deteriorating effect of 2-3 percent points. Small changes in collimator angle gave no changes in conformity, but large changes in collimator angle gave a larger decrease in plan conformity; for angles of 15 and 0 degrees (two arcs, 2.5 mm leaf width), $Q_{0.95–1.05}$ decreased to 75.7% and 71.4%. Consistency between planned and delivered dose was good, with ~92% of measurement points having gamma values <1. Marked deterioration of conformity was seen with positional changes. For 1mm shift in all directions, $Q_{0.95–1.05}$=70%, while for 2mm shift, $Q_{0.95–1.05}$=55.1%.

Conclusions: Results demonstrate that planning of prescription doses with multiple levels for dose painting is feasible using RapidArc, and plans were deliverable. Robustness to positional error was low.

Thursday May 27, 2010

Søren Haack, Aarhus, Denmark

Distribution of low diffusion regions as observed with diffusion weighted MRI in relation to GEC ESTRO targets used for brachytherapy in locally advanced cervical cancer

Haack, S [a], Pedersen, E.M.[b], Jespersen, S.N.[c], Kallehauge, J.F.[d], Lindegaard, J.C.[e], Tanderup, K.[e], *[a] Department of Clinical Engineering; [b] Department of Radiology; [c] Center of Functionally Integrative Neuroscience; [d] Department of Medical Physics and [e] Department of Oncology Aarhus University Hospital, Denmark.*

Introduction: Diffusion Weighted (DW) MRI has the potential for identifying tumor volumes with decreased diffusion indicative for high density of tumor cells. For MRI guided brachytherapy (BT) in cervix cancer, contouring of tumor targets according to GEC-ESTRO guidelines are based on T2 weighted (T2W) images. The objective of this study was to evaluate the distribution of low diffusion volumes determined with DW MRI in relation to anatomically defined GEC ESTRO BT targets (GTV_{BT}, HR CTV and IR CTV).

Materials and Methods: MRI of 9 patients, a total of 13 MRI scans, with locally advanced cervical cancer were performed on a Siemens Symphony 1.5T MR scanner including DWI with b-values at 0, 600 and 1000 s/mm^2. MRI was performed at the time of BT with applicator in place. Contouring was performed based on T2W images (BrachyVision). DW images were subsequently registered to the T2W images. Apparent diffusion coefficient (ADC) maps and mean ADC values for target volumes were calculated. Within the IR-CTV volumes were calculated based on ADC threshold value at $1.2 \cdot 10^{-3}$ mm^2/s.

Results: Mean ADC in GTV_{BT}, (HR CTV ÷ GTV) and (IR CTV ÷ HR CTV) volumes were $1.42 \cdot 10^{-3} \pm 0.47$ mm^2/s, $1.60 \cdot 10^{-3} \pm 0.57$ mm^2/s and $1.81 \cdot 10^{-3} \pm 0.65$ mm^2/s, respectively. Comparison of ADC values for each MRI scan showed that the ADC values inside the HR CTV volume was significantly lower than the ADC values of the surrounding IR CTV volume ($p = 0.019$). No significantly difference was found between the ADC values found inside the GTV_{BT} volume and that of the adjoining HR CTV ($p = 0.256$). For all studies 49.5 % of the calculated ADC volumes were situated inside the HR CTV volume and only 11.0% within the GTV_{BT} volume.

Conclusion: The ADC values were significantly lower in the anatomically defined HR CTV than in the surrounding IR CTV. This could perhaps be utilized for better boundary discrimination between the 2 targets. However, a poor correlation was found between the location of the GTV_{BT} volume and the calculated ADC volume. It seems that the GTV_{BT} volumes do not only contain low diffusion regions and low diffusion regions are also found in the HR-CTV volume, emphasizing the importance of targeting not only the anatomical GTV_{BT}, but the whole HR CTV as recommended by GEC-ESTRO.

Thursday May 27, 2010

Indira Madani, Ghent, Belgium

Adaptive dose painting by numbers for head and neck cancer

Madani I., De Gersem W., Coghe M., Duprez F., De Neve W. *Department of Radiotherapy, Ghent University Hospital, Ghent, Belgium.*

Purpose: To describe the methodology used in the first clinical study on adaptive intensity-modulated radiotherapy (IMRT) applying dose painting by numbers (DPBN).

Materials and Methods: Each patient's treatment used 3 separate treatment plans - fractions 1-10 used a DPBN ([^{18}-F]fluoro-2-deoxy-D-glucose positron emission tomography [^{18}F-FDG-PET]-voxel intensity-based IMRT) plan based on a pre-treatment ^{18}F-FDG-PET/CT scan, fractions 11-20 used a DPBN plan based on a ^{18}F-FDG-PET/CT scan acquired after the 8th fraction and fractions 21-32 used a conventional (homogeneous dose) IMRT plan. Elective neck irradiation was excluded from the conventional IMRT plan. Two dose prescriptions were tested: a median dose of 80.9 Gy to the high-dose clinical target volume (CTV_{high_dose}) [dose level I] and a median dose of 85.9 Gy to the gross tumor volume (GTV) [dose level II]. Dose prescriptions used a linear relationship between ^{18}F-FDG-PET-voxel intensities and dose objectives. Because the three plans used different PET and CT images, dose distributions, dose-volume histograms (DVHs) and indices of biological conformity (Q-volume histograms [QVHs]) were summed after rigid CT- and ^{18}F-FDG-PET image registration. Structure volumes delineated in the pre-treatment ^{18}F-FDG-PET/CT (Approach 1) or per-treatment ^{18}F-FDG-PET/CT (Approach 2) were used to generate summed DVHs and QVHs.

Results: Between February 2007 and August 2009, 7 patients at dose level I and 14 patients at dose level II were treated. Treatment adaptation reduced the volumes for the GTV, CTV_{high_dose}, high-dose planning target volume (PTV) and parotids by 41% (p=0.01), 18% (p=0.01), 14% (p=0.02) and 9-12% (p<0.05), respectively. Depending on the approach, summed doses for all structures differed slightly. Statistical significance was reached for the GTV, CTV_{high_dose}, joint high-dose and elective neck PTV (PTV_{joint}) at dose level I and the CTV_{high_dose}, , PTV_{joint} the expanded spinal cord and brainstem at dose level II.

Conclusions: The adaptive strategy allowed us to modify the treatment using anatomical and biological changes in the targets and organs at risk as detected by ^{18}F-FDG-PET/CT. The in-house developed tools allowed assessment of summed DVHs, QVHs and dose distributions for adaptive treatments.

Thursday May 27, 2010

Frederic Duprez, Ghent, Belgium

A phase I clinical trial on adaptive dose painting by numbers for head and neck cancer: the first clinical results

Duprez F., De Neve W., De Gersem W., Coghe M., Boterberg T., Madani I. *Department of Radiotherapy, Ghent University Hospital, Ghent, Belgium.*

Introduction: A phase I clinical trial on adaptive intensity-modulated radiotherapy (IMRT) using dose painting by numbers (DPBN) was conducted to determine the maximum tolerated dose (MTD).

Material and methods: Treatment of each patient consisted of 2 DPBN plans - fractions 1-10 used a DPBN ([^{18}-F]fluoro-2-deoxy-D-glucose positron emission tomography [^{18}F-FDG-PET]-voxel intensity-based IMRT) plan based on a pre-treatment ^{18}F-FDG-PET/CT scan, fractions 11-20 used a DPBN plan based on a per-treatment ^{18}F-FDG-PET/CT scan - and 1 conventional (homogeneous dose) IMRT plan for fractions 21-32. Two dose escalation levels were tested: a median dose of 80.9 Gy to high-dose clinical target volume (dose level I) and a median dose of 85.9 Gy to gross tumor volume. Any grade 4 toxicity (dose-limiting toxicity) observed during radiotherapy and until 3 months after the treatment end in ≥33% of the patients was a criterion of the MTD. Tumor response was assessed with ^{18}F-FDG-PET/CT at 3 months follow-up.

Results: Between February 2007 and August 2009, 21 patients (17 men, 4 women, age range 46-72, median 60 years) with head and neck squamous cell carcinoma were treated: 7 at dose level I and 14 at dose level II. Nine patients received concomitant cis-platinum-based chemotherapy; 8 patients underwent lymph node dissection prior radiotherapy.
All patients completed treatment without a break. By 3 months follow-up 20 patients were alive, 1 died due to intercurrent disease. No patients presented grade 4 toxicity during treatment and 3 months follow-up, i.e., there was no dose-limiting toxicity. At control ^{18}F-FDG-PET/CT and clinical examination no evidence of disease (NED) was observed in 13/20 patients: 7/7 at dose level I and 10/13 at dose level II, although 4 patients from dose level II had a slight ^{18}F-FDG-avidity inside the dose-escalated region. Partial (>50%) response – local or regional – was detected in 2 patients. In one patient negative clinical examination and ^{18}F-FDG-negativity contested partial (>50%) response detected by CT.

Conclusions: The MTD has not been reached. Given the absence of clinical data on dose-limiting toxicity in dose-painting-by-numbers trials, longer follow-up is warranted to determine the actual MTD in our study.

Thursday May 27, 2010

Anne Kirkebjerg Due, Copenhagen, Denmark

Methodologies for localizing head and neck cancer recurrences in relation to radiation therapy target volumes

Due AK[1], Korreman S[1,2,3], Bentzen SM[1,2], Tomé W[2], Bender E[2], Aznar M[1], Vogelius I[1], Berthelsen AK[1], Kristensen CA[4], and Specht L[4]. *[1]Department of Radiation Oncology, Rigshospitalet, Copenhagen, Denmark. [2]Department of Human Oncology, University of Wisconsin, Madison, Wisconsin, USA. [3] Niels Bohr Institute, University of Copenhagen, Copenhagen, Denmark. [4]Department of Oncology, Rigshospitalet, Copenhagen, Denmark.*

Purpose: To compare methodologies for localisation of head and neck cancer recurrences after radiotherapy, in relation to radiation dose, target volumes and FDG-PET SUV in treatment planning scans.

Patients and methods: Five patients with biopsy-verified local recurrence after IMRT alone or with concurrent chemotherapy for hypopharyngeal SCC were included. All patients had PET/CT scans for radiotherapy planning, and a diagnostic CT scan at the time of suspected recurrence. Retrospectively, the recurrence volume was delineated in the follow-up scans by a radiologist, and within this volume putative points of origin of the recurrence was determined by 3 strategies; defined by an oncologist, as the centre-of-volume, and by volumetric contraction. The recurrence volume and points of origin were propagated to the treatment planning scan, and the relations to target volumes, radiation doses and PET SUV were quantified.

Results: Three out of five patients had <50% of the propagated recurrence volume included in the PET positive volume and two out of five had <50% overlap with GTV volumes. For the same three/two patients were the locations of the points of origin outside the PET positive/GTV volumes. For all patients, there was >55% overlap between the recurrence volume and the elective target volumes. All points of origin were located within the PTV-T, receiving more than 100% of prescription dose. The distances between points of origin were <6 mm in three of out five patients, while for one patient the volume-contraction point differed more. In the fifth case, the oncologist defined two points of origin. PET-SUV ranged from 2.85 to 20.71 – for each patient, the variation in PET-SUV for the points-of-origin was up to 30% (except the out-lying volume contraction point, with difference >100%).

Conclusions: There was good correspondence between recurrence/target volume overlap and point of origin locations in relation to target volumes, such that the location of the points-of-origin with respect to target volumes corresponded with a volume overlap threshold of 50% of the recurrence volume. Several patients had small volume overlap between recurrence and PET positive/GTV volumes, and points of origin correspondingly located outside these target volumes. All five patients had the points of origin located in the high-dose region.

Thursday May 27, 2010

Session 4: Imaging of normal tissue function

Yue Cao, Ann Arbor, USA

Functional Imaging as a Biomarker for Radiation-Induced Normal Tissue and Organ Toxicity

Yue Cao, Ph.D. *Departments of Radiation Oncology and Radiology, University of Michigan, USA.*

Radiation therapy (RT) is a major treatment modality for malignant tumors. The major limiting factor is radiation-induced normal tissue and organ toxicity. Clinical symptoms usually occur delayed or late as weeks and months after the completion of RT. The clinical outcome ranges from mild, reversible damage to death. In the past, efforts to develop models to estimate the likelihood of developing radiation-induced organ toxicity have been based primarily on the planned radiation dose distribution and dose fraction size in the organ of interest. These analyses have demonstrated their usefulness for permitting the safe delivery of higher doses of radiation than have previously been possible. However, there is a broad range of individual patient sensitivity that is not reflected by predictions made solely based on the physical dose distribution or general clinical features. If individual patient sensitivity could be better estimated before or during a course of treatment, it would permit higher doses of radiation to be delivered safely to the tumors of patients who is relatively radiation resistant, thus prolonging survival without increasing complications. It would be valuable to identify biomarkers, including those derived from in vivo imaging, for early assessment of individual sensitivity to radiation and prediction of late normal tissue and organ toxicity. Such biomarkers might provide an opportunity to individualize the dose of RT. Our group has been conducting active research in this area. Our results will be summarized in the presentation. Examples from brain, liver and head and neck will be given.

Thursday May 27, 2010

Mike Partridge, Sutton, UK

The Imaging of Normal Tissue Function in Lung Radiotherapy

Dr Mike Partridge, *The Institute of Cancer Research, Sutton, UK.*

There is growing clinical evidence that functional imaging is useful for target volume definition and early assessment of tumour response to external beam radiotherapy. A subject that has perhaps received less attention, but is no less promising, is the application of functional imaging to the prediction or measurement of acute radiation injury to normal tissues. In this abstract the currently published literature describing the use of functional imaging of normal tissues in radiotherapy for lung cancer is reviewed.

Patients with non-small cell lung cancer often present with compromised lung function, either as a direct result of the tumour, or due to co-existent disease. The use of single photon emission computed tomography of ^{99m}Tc-labelled macro-aggregated albumin (^{99m}Tc-MAA SPECT) has been widely reported for visualising patterns of lung perfusion. When registered with planning CT data, 3D conformal treatment plans have been shown which reduce dose to healthy lung particularly for patients with large localised perfusion deficits. The use of intensity-modulated beam delivery has been shown to be capable of further reducing dose to the functioning lung. Imaging of lung ventilation and its application to radiotherapy planning has also been demonstrated using hyperpolarised ^{3}He magnetic resonance imaging (^{3}He MRI), yielding broadly similar results to those obtained with ^{99m}Tc-MAA SPECT.

If dose to functioning lung is shown to be the primary cause of lung toxicity, the combination of functional imaging and IMRT may allow dose escalation by specific avoidance of functioning lung. For patients with highly compromised pre-radiotherapy breathing function, preservation of remaining functioning lung may also reduce some of the risks associated with radical treatment. However, accurate knowledge of the dose-response of lung tissue as a function of perfusion (or ventilation) is still unclear. Clinical and experimental evidence is emerging showing that dose-dependent reductions in regional lung perfusion can be observed and weak associations between integrated response and whole lung function have been reported. Before widespread clinical implementation of such a technique, further research is required to allow better selection of which patients would gain most clinical benefit from image-guided functional-lung avoidance.

Published results to date demonstrate that the use of functional imaging to preferentially avoid normal lung tissue not easily identifiable on solely anatomical images is technically feasible: this gives the potential to reduce toxicity. Functional imaging has also been shown to be a potentially powerful tool for the early detection of radiotherapy-induced normal tissue injury. Improved clinical evidence of the link between radiation-induced changes in perfusion imaging and clinically relevant pulmonary function would be beneficial for patient selection and treatment optimisation.

Thursday May 27, 2010

Morten Høyer, Aarhus, Denmark

Functional imaging of the liver using 18-Fluoro-Deoxy-Galactose and PET7CT scanning. Implications for planning of SBRT for liver tumours.

Morten Høyer, Michael Sørensen, Jørgen BB Petersen, Ludvig P Muren, Marianne Ingerslev Holt, Susanne Keiding. *Aarhus University Hospital, Aarhus, Denmark.*

Objectives: Radiation induced liver disease (RILD) is a severe, however seldom, morbidity following radiotherapy (RT) for liver tumors (1). Based on sparse knowledge on the development of RILD, clinicians tend to be conservative in selection of patients with liver tumours suitable for stereotactic body RT (SBRT). Various constraints have been suggested and sparing of at least 700 cc of normal liver tissue to a radiation dose less than 15 Gy is widely used. There are no standard methods for determination of spatial metabolic function of the liver and so far all constraints are based on volumes assuming homogenous organ function, disregarding any spatial patterns in pre-treatment function of the liver. We have developed a PET/CT method using the positron labelled galactose tracer ^{18}fluoro-deoxy-galactose, ^{18}FDGal, to determine spatial metabolic liver function (2). Galactose elimination from the blood is a standard measurement of the global liver function in patients with liver disease. Here we present preliminary results of ^{18}FDGal PET/CT in 5 patients treated with SBRT and results of a treatment planning study utilizing the PET-data.

Methods: A dynamic ^{18}FDGal PET/CT recording was performed before, 1 month and 3 months after SBRT of liver tumors. Conventional contrast-enhanced CT-scanning was acquired simultaneously. Hepatic metabolism of ^{18}FDGal was quantified and a treatment planning study using IMRT with conventional constraints to liver, lung, intestine and spinal cord as well as constraints based on the ^{18}FDGal PET/CT was performed.

Results: Uptake of ^{18}FDGal was clearly reduced in liver tissue exposed to radiation. The relative reduction in ^{18}FDGal uptake in liver exposed to doses higher than 30 Gy ranged from 66-40%. The reduction in uptake was a linear function of RT dose. Moreover the treatment planning study showed that addition of constraints from ^{18}FDGal PET/CT enabled sparing of the liver with highest ^{18}FDGal uptake, i.e. highest metabolic function.

Conclusion and perspectives: Preliminary results from 5 patients strongly indicate that the method accurately estimates the spatial metabolic function of the liver and the radiation induced reduction in metabolic function. It also shows that treatment planning based on ^{18}FDGal PET/CT scanning is feasible.

1. Høyer-M et al.: Phase II study on stereotactic body radiotherapy of colorectal metastases. Acta Oncol 45: 823-830, 2007.
2. Sørensen-M et al. Hepatic uptake and metabolism of galactose can be quantified in vivo by 2-[18F]fluoro-2-deoxygalactose positron emission tomography. Am J Physiol Gastrointest Liver Physiol 295: G27–G36, 2008.

Thursday May 27, 2010

Session 5: Functional imaging segmentation, registration and quantification

Marc Kessler, Ann Arbor, USA.

Tools of our trade: segmentation and registration for planning, delivery and adaptation

Marc L Kessler, PhD. *The University of Michigan Medical School, Department of Radiation Oncology, Ann Arbor, Michigan, USA*

Acquisition and processing of medical image data are now fundamental parts of patient management in radiation therapy. Image data are used to aid diagnosis and staging, to guide treatment planning and delivery and to help monitor the patient during and after therapy. Most radiotherapy departments have dedicated CT scanners, some with 4D capabilities. Many departments also have or are contemplating dedicated MR and PET/CT scanners. More imaging devices are also appearing in the treatment room, with in-room, on-board and integrated imaging devices becoming commonplace. The availability of hybrid MR scanner/treatment units is also not far off.

In order to leverage the plethora of anatomic, functional and time series data available, effective processing tools are needed to extract useful information and to combine and present it in a way that promotes a clear and efficient workflow. The typical radiotherapy imaging toolkit now includes a broad range of basic tools such as image enhancement, n-D visualization, segmentation, registration and quantification. These tools may be used individually or in combination at many points in the radiotherapy process with the overall goal to create a more accurate and complete model of the patient so that an effective course of therapy can be devised, delivered and adapted as needed.

In this presentation, an overview of the various image processing tools and techniques used to segment, register, combine and analyze the information from a set of imaging studies will be presented. Use of these tools at several steps of the radiotherapy process will be described and elucidated using clinical examples.

Thursday May 27, 2010

Thea Sollien, Oslo, Norway

Histogram analysis of pharmacokinetic parameters derived from dynamic contrast enhanced imaging

Sollien T, Andersen EKF, Hagtvedt T, Seierstad T, Geier OM, Malinen E. *The Norwegian Radium Hospital, Oslo University Hospital, Oslo, Norway.*

Introduction: This study presents a methodology for systematic evaluation of intratumoral distribution of pharmacokinetic parameters derived from dynamic contrast enhanced imaging. The results are compared with those obtained from conventional pharmacokinetic analysis using mean tumor uptake.

Materials and methods: Twenty-two patients with malignant lymphoma and 15 controls underwent dynamic contrast enhanced CT. Time-enhancement curves in malignant and normal lymphoid tissue were fitted voxel by voxel to a generalized pharmacokinetic compartment model. The fitting provided estimates of the volume transfer constant (K^{trans}), the relative volume of the extravascular extracellular space (n_e) and the transit time of contrast agent (t_0). Histograms were obtained from the intratumoral parameter distribution for each case. From the histograms, the 1^{st} to the 99^{th} percentile was extracted for each parameter. Using logistic regression analysis, the dependence of the binary variable (patient/control) on the n^{th} percentile was elucidated. A significance level of 0.05 was employed.

Results: The P-value from the logistic regression was strongly dependent on the percentile under consideration for a given pharmacokinetic parameter. For n_e and t_0, bands of significance were found at certain percentile intervals. For some bands, patients had on average higher parameter values than the controls, while the opposite was found for other bands. Conventional analysis gave a significant difference between patients and controls for K^{trans} and t_0.

Conclusions: Systematic screening of intratumoral distribution of pharmacokinetic parameters from dynamic contrast enhanced imaging may provide information not obtainable from conventional analysis using whole tumor uptake.

Thursday May 27, 2010

Erland Andersen, Oslo, Norway

Histogram-based segmentation of regions at risk in cervical cancers by dynamic contrast enhanced MRI and pharmacokinetic modeling

Andersen EKF[1], Hole KH[2], Lund KV[2], Sundfør K[3], Kristensen GB[3], Lyng H[4], Malinen E[1]. *[1]Department of Medical Physics/ [2]Department of Radiology/ [3]Section for Gynaecological Oncology/ [4]Department of Radiation Biology. The Norwegian Radium Hospital, Oslo University Hospital, 0310 Oslo, Norway.*

Introduction: Dynamic contrast enhanced MRI (DCE-MRI) allows for non-invasive characterization of vascular properties of tumors. The aim of this study was to develop a method to identify radioresistant regions at risk in cervical cancer patients using DCEMRI, pharmacokinetic modelling and histogram analysis.

Materials and methods: Eighty-four patients with locally advanced cervical cancer treated with chemoradiotherapy were included. The median follow-up time was four years. Sixteen patients had locoregional relapse. All patients underwent DCE-MRI with Gd-DTPA before treatment. The DCE-MR-images were analyzed using a pharmacokinetic model providing estimates of the maximum amount of contrast agent contained in a voxel (A), the transfer constant between blood plasma and interstitium (k_{ep}) and the clearance rate of contrast agent from the voxel (k_{el}). For each patient and pharmacokinetic parameter, the intratumoral parameter distribution was stored as a frequency histogram. By assuming that parameter values signifying radioresistance occur more frequent in patients who did not respond to treatment, the dependence of the histogram frequencies on the treatment outcome were evaluated by logistic regression for each parameter.

Results: An interval of k_{ep} values were positively correlated with locoregional relapse. For this interval, non-responders had increased histogram bin frequency compared to responders. Tumor voxels with k_{ep} values in that interval were classified as regions at risk in the MR-images. Kaplan-Meier curves for patients with high and low fraction of k_{ep} values showed a significant difference in risk of locoregional relapse (log-rank p-value: < .001). There were no significant relationship between the parameters A and k_{el} and treatment outcome.

Conclusions: Analysis of pharmacokinetic histograms derived from DCE-MRI may identify regions at risk in cervical cancer patients. However, pathological validation of the segmented regions is required.

Thursday May 27, 2010

Session 6: Quantitative analysis and modelling of clinical outcome

Eirik Malinen, Oslo, Norway

TCP modeling of biological image guided radiotherapy

Malinen E[1], Søvik Å[1,2], Olsen DR[3]. *[1]Department of Medical Physics, The Norwegian Radium Hospital, Oslo University Hospital, Norway. [2]Department of Companion Animal Clinical Sciences, Norwegian School of Veterinary Science, Oslo, Norway. [3]Faculty of Mathematics and Natural Sciences, University of Bergen, Norway.*

Introduction: Tumors may be heterogeneous with respect to radiosensitivity, and a homogeneous tumor dose is thus not always optimal. In biological image guided radiotherapy, medical images of radiobiological relevance are used to guide focal irradiation of solid tumors. Tumor control probability (TCP) modeling may be useful for estimating the effect of biological image guided radiotherapy.

Materials and methods: A TCP model based on the linear quadratic cell survival formalism has been developed. The model requires 3D mapping of tumor radiosensitivity and absorbed dose. Optimizing TCP under the constraint of constant integral tumor dose, optimal dose prescription maps may be obtained. The set of optimal doses may be used as input for dose-based inverse planning of intensity modulated radiotherapy. TCP calculations based on both the optimal set of doses and the dose distribution from IMRT planning could thus be performed. A canine hypoxia tumor model and an IMRT planning system was used to for showing the potential benefit from biological image guided radiotherapy. Additional aspects such as replanning, set-up uncertainties and utilization of high-LET particles will be discussed.

Results: TCP following biological image guided radiotherapy was considerably improved compared to that following conventional radiotherapy with the same integral tumor dose. However, the dose distributions from IMRT planning gave reduced TCP compared to the optimal dose prescription, indicating that improvements in dose delivery are warranted.

Conclusions: TCP modeling of biological image guided radiotherapy is useful, providing that the image basis reflect the true underlying radiobiological profile and that highly focal dose distributions can be accurately delivered.

Thursday May 27, 2010

Joseph Deasy, St.Louis, USA

Normal Tissue Complication Probability (NTCP) Modeling Of Late Rectal Bleeding Following External Beam Radiotherapy For Prostate Cancer: A Test Of The QUANTEC-Favored Model and the Implications for Treatment Planning.

M. Liu1, V. Moiseenko2, A. Agranovich1, A. Karvat1, W. Kwan1, Z. Saleh3, A. Apte3, J. Deasy3, 1*) Fraser Valley Centre, British Columbia Cancer Centre, Surrey, BC, Canada, 2) Vancouver Centre, British Columbia Cancer Agency, Vancouver, BC, Canada, 3) Mallinckrodt Institute of Radiology, Washington University, St. Louis, MO.*

Purpose/Objective(s): We test the NTCP model recommended by QUANTEC (quantitative analysis of normal tissue effects in the clinic) against an independent dataset. We further discuss the implications for routine treatment planning of NTCP model uncertainties.

Materials/Methods: 161 prostate cancer patients were treated with 3D conformal radiotherapy at the British Columbia Cancer Agency.

Results: Out of the 161 patients, 12 (7.5 %) had late rectal bleeding of Grade >= 2. Multivariate logistic regression showed a poor correlation between dose-volume parameters (V60, V70, etc.) and late rectal bleeding. Bootstrap refit LKB model parameters had positively skewed distributions with peak values and 95% confidence intervals of: n = 0.08 (0-10); m = 0.08 (0.02, +infinity); and TD50 = 76 (71, +infinity) Gy. However, on this dataset, both models poorly predicted late rectal bleeding: the best-fit LKB model had a non-significant Spearman correlation coefficient of 0.098 (p=0.11); and the QUANTEC model had a coefficient of 0.096 (p=0.11). The effect of uncertainties in NTCP models for typical treatment plans is also investigated using simulations.

Conclusions: The observed rectal bleeding dose-volume response is in a broad agreement with the QUANTEC recommendations. However, both the QUANTEC-preferred LKB model parameters and the best-fit LKB model parameters yield poor predictive power in this dataset. We conclude that the QUANTEC-preferred LKB model may not reliably correlate to the risk of late rectal bleeding, at least for the types of treatments considered here.

Partially supported by NIH grant R01 CA85181.

Thursday May 27, 2010

Iuliana Toma-Dasu, Stockholm, Sweden

Dose painting by numbers - are the practical limitations of the technique decreasing or increasing the probability of controlling the tumour?

Toma-Dasu I[1]**, Daşu A**[2]**.** [1] *Medical Radiation Physics, Stockholm University and Karolinska Institutet, Stockholm, Sweden. Department of Radiation Physics, Linköping University Hospital, Linköping, Sweden.*

Introduction: Ever since the dose-painting-by-numbers concept was introduced several questions regarding its limitations for treatment planning were raised including the implications of the resolution of the imaging technique used and the accuracy of the resulting heterogeneous dose distributions. This study aims to assess the impact of the image resolution and the resulting heterogeneity of the dose distribution implied by dose-painting-by-numbers on the probability of controlling dynamic tumours.

Methods and Materials: H&N cancer patients were planned with a dose-painting-by-numbers technique based on FMISO-PET images. The advantages and disadvantages of this method for calculating the dose to be delivered to the hypoxic regions as an integrated boost have been theoretical investigated in terms of the predicted tumour control probability (TCP). Several levels of resolution of the images used to assess the resistance of the tumour that would lead to different levels of heterogeneity in the dose-painting-by-numbers plan have been assumed.

Results: Assuming a dynamic tumour oxygenation during the course of fractionated radiotherapy, a very fine heterogeneous dose distribution ideally calculated at voxel level for a 90% TCP would fail to control the tumour. Mismatches between the hotspots in the dose distribution and the resistant hypoxic foci could lead to a loss in TCP as high as 70%. Only adaptive treatment compensating for the loss of control by a general increase in dose would lead to reasonably high TCPs. The results also show that coarse image resolutions and the resulting dose distributions might compensate for microscale mismatches, but the resulting tumour control could still be as low as 10% below the target TCP.

Conclusions: The clinical success of current approaches for dose-painting-by-numbers in the absence of adaptive approaches might be explained by changes in tumour radiation resistance though reoxygenation.

Thursday May 27, 2010

Pauliina Wright, Oslo/Aarhus, Norway/Denmark

Evaluation of adaptive radiotherapy of bladder cancer using image-based tumour control probability modelling

Pauliina Wright[1,2,3], Ludvig P Muren[1,2], Morten Høyer[2], Eirik Malinen[3]. *[1]Department of Medical Physics, Aarhus University Hospital, Denmark. [2]Department of Oncology, Aarhus University Hospital, Denmark. [3]Department of Medical Physics, The Norwegian Radium Hospital, Norway.*

Introduction: Clinical implementation of adaptive radiotherapy strategies could benefit from extended tools for plan evaluation and selection. For this purpose we have investigated the feasibility of tumour control probability modelling (TCP) using the bladder as example of a tumour site with potential benefit from adaptive strategies.

Materials and Methods: Two bladder cancer patients that underwent planning CT and daily cone beam CT imaging during the treatment course were included. The bladder was outlined in every image series. Following a previously published procedure, various adaptive planning target volumes (PTVs) were generated from the inter-fraction bladder variations during the first five imaging sessions. Intensity-modulated treatment plans delivering 60 Gy to a given PTV were generated. In addition, simultaneous integrated boost (SIB) plans giving an additional dose of 10 Gy to the tumour were created. Using the daily cone beam CT images and polynomial warping, the dose in each bladder volume element was tracked fraction by fraction. TCP estimates employing the accumulated dose distribution in the bladder and realistic radiosensitivity parameters were produced. The dependence of TCP on the simulated clonogenic cell distribution was explored.

Results: For a uniform clonogenic cell density in the whole bladder, TCP varied between 53-58% for the 60 Gy plans, while it was 51-64% for the SIB plans. The lowest values corresponded to the smallest PTVs, not enclosing the target on all fractions. Increasing the clonogenic cell density in the tumour relative to that in the remaining bladder, TCP saturated at approximately 76% for the SIB plans.

Conclusion: Dose tracking and TCP calculation provided additional information to standard criteria such as geometrical coverage for the selected cases. TCP modelling may be a useful tool in plan evaluation and for selection between multiple plans.

Thursday May 27, 2010

Ivan S.Vogelius, Copenhagen, Denmark

Risk of radiation pneumonitis is insensitive to hypofractionation with modern conformal radiation delivery techniques

Vogelius, IS, PhD*§, Westerly, DC, PhD†, Cannon, GM, MD†, Mackie, TR, PhD†, Mehta, MP, MD†, Bentzen, SM, PhD, DSc†. *†Department of Human Oncology, University of Wisconsin School of Medicine and Public Health, Madison, WI 53792, USA. * Department of Oncology, Vejle Sygehus, 7100 Vejle, Denmark. § Department of Radiation Oncology, Rigshospitalet, Denmark.*

Purpose: To explore the effect of hypofractionated conformal radiotherapy on the risk of radiation pneumonitis (RP) as estimated from normal tissue complication probability (NTCP) models.

Methods and materials: Eighteen non-small cell lung cancer patients previously treated with helical tomotherapy were selected for this study. The standard fractionation was set to 60 Gy in 30 fractions. Iso-effective comparisons with hypofractionation were performed by changing the fractionation and the physical prescription dose while keeping the equivalent tumor dose in 2 Gy fractions constant. The risk of developing RP was estimated using the mean lung dose (MLD) model of NTCP using the local equivalent dose in 2-Gy fractions with α/β= 4 Gy for the residual lung and compared to the risk with standard fractionation. The total treatment time was kept constant.

Results: The mean risk of clinical RP at the standard fractionation is 7.6% for the Tomotherapy plans (range: 2.8-15.9 %) and 9.2% for the 3D-CRT plans (range 3.2-20.2%). Changing to 20 fractions we find that the Tomotherapy plans become slightly less toxic if the tumor α/β=7 Gy (mean RP risk 7.5%, range 2.8-16%) while the 3D-CRT plans become marginally more toxic (mean RP risk 9.8%, range 3.2-21%). In this case the Tomotherapy plans are favored because a major contribution to the MLD stems from the extensive low dose bath. At low doses, the biological effective dose decreases with hypofractionation because the decrease in physical dose is more important than the fraction size. If the tumor α/β is 13 Gy, the mean estimated risk of RP is 7.9% for Tomotherapy (range: 2.8-17%) and 10 % for 3D-CRT (range 3.2 – 22 %).

Conclusions: Modern conformal radiotherapy techniques facilitate hypofractionation of NSLC with little if any increase in the estimated risk of RP. A clinical benefit may be achievable from accelerated fractionation and/or if the tumor α/β is moderately low.

Thursday May 27, 2010

Tine Schytte, Odense, Denmark

Mean radiation dose to the heart and risk of cardiac toxicity in NSCLC treated with definitive radiotherapy

Tine Schytte, Olfred Hansen, Thomine Stolberg-Rohr* and Carsten Brink*. *Department of Oncology and Radiophysic Laboratory* Odense University Hospital, Denmark.*

Background: Lung and oesophageal toxicity have been regarded as main toxicity in definitive radiotherapy (RT) of non-small cell lung cancer (NSCLC), whereas cardiac toxicity has not been offered much concern. This is probably due to the poor prognosis for patients with unresectable NSCLC. In this study we report the heart toxicities in NSCLC patients (pts) treated with RT in our centre.

Methods and material: Cardiac toxicity is defined as having a cardiac event either as myocardial infarction (MI), pericardial effusion, cardiac insufficiency (CI), pulmonary embolism (PE), found dead with unknown cause, non specific cardiac disease (CD), supra- or ventricular arrhythmia (SA, VA). The cardiac events (CE) were collected from patient files. From 01.09.1995-28.02.2007 pts with NSCLC (stage I-IIIB and recurrent disease) were treated with RT at our centre with planned dose 60-80 Gy. All RT was applied as 3D-RT in 2 Gy/F without elective nodal irradiation. All patients were followed to death. Median follow-up was 95 months with 36 month as a minimum. In each patient the heart was delineated in following volumes: Left ventricle, both ventricles and the whole heart. Mean dose was calculated for each volume in the treatment plan.

Results: 72 patients had cardiac disease prior to RT. They are excluded from the following analysis. Pts treated with concomitant chemotherapy (9 pts) were excluded as well. 34 pts had a CE: 9 AMI, 5 CI, 2 PE, 3 found dead with unknown cause, 2 CD, 13 SA and 1 VA, 1 pericardial excaudate. In 7 pts it was uncertain whether there was a cardiac disease. Median survival was 17.2 month and overall survival for 1, 2 and 5 year was 65%, 37% and 15%, respectively. High mean dose (≥upper quartile) to left ventricle (14.45 Gy), both ventricles (17.2 Gy) or whole heart (24.7 Gy) was not correlated with having a CE.In a Cox-regression analysis of time to CE, induction chemotherapy, high mean dose to left + right ventricles, > 65 year, poor PS and high lung V20 were not a statistically significant factors whereas gender were.

Discussion: We did not find any correlation between high mean dose to the heart and having a CE. The occurrence of CE did not influence the overall survival.

Thursday May 27, 2010

Maria Thor, Aarhus, Denmark

Rectum motion and morbidity prediction: Improved correlation between late morbidity and DVH parameters for rectum planning organ at risk volumes

Thor M[1, 2], Væth M[3], Karlsdottir À [4], Muren LP [1, 2,4]. *[1]Departments of Oncology and Medical Physics, Aarhus University Hospital. [2]Clinical Institute, Aarhus University. [3]Department of Biostatistics, Aarhus University. [4]Department of Oncology and Medical Physics, Haukeland University Hospital, Bergen, Norway.*

Introduction: The rectum is a major dose-limiting organ at risk (OR) in radiotherapy (RT) of prostate cancer. The ability to predict adverse effects in the rectum is therefore essential, but the precision of present predictive approaches is limited by the internal motion of this organ. In this study late rectal morbidity is investigated in relation to the internal motion of the rectum applying a population-based measure of motion, the ICRU 62 'Planning organ at Risk Volume' (PRV) concept.

Material and methods: Late rectal morbidity was analysed in 242 prostate cancer patients treated to 70 Gy with conformal RT either to the prostate, the prostate and seminal vesicles or the whole pelvis (initial 50 Gy only). Our late rectal morbidity endpoint was defined as the maximum recorded grade classified by the late gastro-intestinal (GI) RTOG toxicity scoring system. Patients were stratified into two groups: Grade 0-1 and Grade 2 or higher. Cumulative dose-volume histograms (DVHs) were derived for the rectum OR and six rectum PRVs *i.e.* the OR extended with six different margins (narrow/intermediate/wide in anterior direction or in both anterior and posterior direction). The difference in rectum dose-volume parameters between patients with Grade 0-1 vs. Grade 2 or higher was investigated by logistic regression and permutation tests.

Results: Late Grade 2 or higher toxicity was observed in 25 of 242 (10%) patients. The irradiated fractional rectum volume for these patients was on average 2% larger for high (62-73 Gy) and 5% larger for intermediate (37-42 Gy) dose levels. The logistic regression analysis as well as the permutation tests reached significance ($p \leq 0.05$) for only one dose level for the rectum OR (40 Gy). For the PRVs, a range of dose levels were found to be significant (p-value range: 0.01-0.046), most pronounced for the PRV with margins of 6 mm anterior and 5 mm posterior (PRV 4) with 10 significant high (62-71 Gy) and 5 intermediate dose levels (38-42 Gy) (Figure 1). The average area under the DVH curve for this PRV across the significant dose levels was 188 respectively 170 for patients with Grade 2 or higher vs. Grade 0-1 toxicity for the high and 70 respectively 62 for the intermediate dose levels.

Conclusion: The statistical methods applied displayed consistently a small, though significant, difference in DVH parameters between patients with vs. without Grade 2 or higher late rectal morbidity for intermediate and high dose levels. The difference became far more evident when using a PRV with narrow margins.

Friday May 28, 2010

Session 7: Adaptive strategies and technologies

Karin Haustermans, Leuven, Belgium

How to adapt the multimodal treatment in rectal cancer based on imaging?

Karin Haustermans, MD, PhD, Maarten Lambrecht MD. *Department of Radiation Oncology, Leuven Cancer Institute, UZ Gasthuisberg, Leuven, Belgium.*

Introduction: The addition of preoperative chemoradiation (RCT) to surgery has decreased locoregional recurrence rates in patients with rectal cancer. The advantage of using RCT followed by a 6-8 week rest period before surgery is that this approach allows for significant tumor downsizing with 10-30% of the patients showing a pathologic complete response (pCR) at the time of surgery. Some studies suggest that surgery can be omitted in patients with a clinical complete response leading to organ preservation in this disease. Predicting response to treatment before or early during RCT would allow for a patient tailored treatment.

Material and methods: An FDG-PET/CT and a DW-MRI were performed, prior to RCT, after 10-12 fractions and 5 weeks after the end of RCT. Lesions were delineated using a gradient based delineation method and the maximal standardized uptake values (SUVmax) were determined for each region of interest (ROI). In all patients a DW-MRI with 6 b-values between 0 and 1000 s/mm2 was performed at the same time points. A region of interest was delineated on the b1000 images. Mean apparent diffusion coefficients (ADC) were determined. Tumor response was scored on the resected specimen according to the ypTNM classification. Findings on pathology were correlated with changes in SUVmax during and after preop RTC, the initial ADC value, the percentage volume reduction (ΔV) and the change in ADC value (ΔADC) between baseline and the follow-up scans. Receiver-operating characteristics (ROC) analysis with the area under the curve (AUC) was used to investigate the discriminatory capability of the parameters.

Results: Both the ΔSUVmax during and after RCT were significantly correlated with the pathological response to treatment (During: ΔSUVmax = 56% ± 10 for pCR vs 29% ± 20 if no pCR, p: 0.0057; Post: ΔSUVmax = 89% ± 13 for pCR vs 64% ± 20 if no pCR, p: 0.0167). Using ROC curve analysis, an optimal threshold for ΔSUVmax of 40% is able to assess pCR with a sensitivity of 100% and a specificity of 69%. After RCT a threshold value for ΔSUVmax of 73% was able to assess all pCR with a sensitivity of 100% with a specificity of 75%. The initial ADC value was also significantly correlated with the pathological response after preoperative treatment (0,94 ± 0,12 x 10-3 mm^2/s for pCR vs 1,2 ± 0,24 x10-3 mm^2/s, p = 0,0020) and an optimal threshold of 1.06 x 10-3 mm^2/s yielded a sensitivity of 100% with a specificity of 88%. The mean ΔV during and after RCT was significantly higher in patients with pCR compared to patients without (ΔVduring = -62% ± 16 vs -33% ± 16 respectively; p=0.015 and ΔVpost= 86% ± 12 vs 60% ± 21; p = 0.012). ROC curve analysis revealed an optimal threshold for ΔVduring of -45% during RCT (sensitivity: 83% and specificity: 71%) and -77% for ΔVpost (sensitivity 83% and specificity 86%).

DW-MRI during and after RCT showed a significantly higher ΔADC in patients that reached pCR compared to patients without a pCR (during RCT: 72% ± 14 versus 6% ± 12; p=0.0006 and after RCT: 88% ± 35 vs 26% ± 19; p = 0.0011). An optimal threshold for ΔADC during RCT of 50% was able to accurately separate patients reaching a pCR from other patients (sensitivity and specificity of 100%). After RCT a threshold for ΔADC of 48% yielded a sensitivity of 100% and a specificity of 93%.

Conclusion: FDG-PET and DW-MRI can be used in rectal cancer to predict the response to pre-operative RCT.

Friday May 28, 2010

Richard Pötter, Vienna, Austria

Is repetitive morphologiC imaging valuable for Bigart? – Experience from MRI based adaptive cervix brachytherapy (GynART)

Richard Pötter, MD, Maximilian Schmid, MD, Barbara Bachtiary, MD, Johannes Dimopoulos MD. *Medical University of Vienna, General Hospital of Vienna, Austria.*

Since long it has been recognized in cervix cancer treatment that clinical morphologic response during and at the end of radio (chemo) therapy is a strong predictor for final tumour control. In particular, large tumours with poor response seem to have a worse prognosis as compared to well responding tumours (Huang et el. 2010).

This clinical observation has been further elaborated by MRI based morphologic imaging studies which showed that tumours with poor response and/or incomplete remission were frequently associated with progressive (locoregional) disease whereas tumours with good partial remission at the end of external beam radiotherapy/brachytherapy had a favourable outcome (Flueckiger et al. 1992).

With the upcoming MRI based brachytherapy, repetitive MR imaging was introduced on a regular basis, addressing the pattern of spread at diagnosis and at the time of brachytherapy after 40-45 Gy radio(chemo)therapy. Three types of response could be identified in 103 patients: exophytic tumours with high partial response rates, mixed exophytic/infiltrative tumours with intermediate response rates, infiltrative tumours with poor response rates (Dimopoulos et al. 2008). Quantitative assessment showed in 49 patients overall a volume remission rate of 75%, with a mean tumour volume of 61 ccm at diagnosis and of 16 ccm at the time of brachytherapy. The mean volume at the end of brachytherapy was 8 ccm (Dimopoulos et al. 2009).

Large volume at diagnosis, often associated with significant residual disease at the time of brachytherapy (indicating poor or intermediate response) was associated with poor outcome (36% 3y local recurrence rate in 40 patients) in the early phase of MRI based brachytherapy in Vienna (1998-2000, Pötter et al. 2007).

Volume and dose adaptation/escalation through combined endocavitary/interstitial techniques and MRI based volume adaptation and dose escalation could significantly reduce the local recurrence rate in the following years to a 18% 3 year local recurrence rate in 38 patients (2001-2003, Pötter et al. 2007) and to a 6% 3 year local recurrence rate in overall 97 patients (2001-2008: unpublished material).

These morphologic imaging findings indicate that it seems to be possible to identify unfavourable patient subgroups through repetitive morphologic imaging, which profit from dose and volume adaptation/escalation through a risk adapted brachytherapy boost.

These findings imply that a thorough understanding of repetitive morphologic imaging in a given solid squamous cell cancer setting can represent a solid and comprehensive basis for identifying prognostic unfavourable subgroups which may profit from local treatment adaptation. In addition to such repetitive morphologic imaging, biologic repetitive imaging may help to elaborate further on the definition of prognostic unfavourable subgroups and to add further predictive and/or prognostic overall information on local/regional/distant disease outcome. A prospective study from Vienna in a limited number of cervix cancer patients (n=14) investigating repetitive FAZA PET will provide some data to support this suggestion.

Friday May 28, 2010

Anne Vestergaard, Aarhus, Denmark

Adaptive strategies for radiotherapy of bladder cancer – a feasibility study

Anne Vestergaard[1], Jimmi Søndergaard[2], Jørgen BB Petersen[1], Pauliina Wright[1, 2, 3], Morten Høyer[2] and Ludvig P Muren[1, 2]. *[1]Department of Medical Physics, Aarhus University Hospital, Nørrebrogade 44, DK-8000 Aarhus C, Denmark. [2]Department of Oncology, Aarhus University Hospital, Nørrebrogade 44, DK-8000 Aarhus C, Denmark. [3]Department of Medical Physics, The Norwegian Radium Hospital, Ullernchausseen 70, 0310 Oslo, Norway.*

Introduction: Bladder cancer patients show considerable individual variation in target position and volume during a course of Radiotherapy (RT). We have developed three different adaptive RT (ART) methods involving daily plan selection using cone beam CT (CBCT). In this study we compare the performances of these three methods relative to standard, non-adaptive RT.

Materials and methods: Ten patients treated for bladder cancer in our department underwent daily CBCT and bony anatomy match. Seven of the patients were treated with a simultaneous integrated boost (SIB) to the bladder (60 Gy) and the pelvic lymph nodes (48 Gy). Three patients received 60 Gy in 30 fractions to the bladder. Retrospectively, we compared three ART strategies based on daily selection of the most suitable plan from a library consisting of three IMRT-plans corresponding to a small, medium and large target volume. ART Method A used population based margins from CTV (Clinical Target Volume, here the bladder) to Plan Selection Volume (PSV), which is used to select the dose plan on a daily basis. In Method B the margins from CTV to PSV are based on a scoring of the directions, where the CBCT bladder extents outside the plan CT bladder, as observed in the first five fractions. Volumes for Method C are based on the delineations of the bladder on the planning CT and the first four CBCT-scans. The total dose distribution was calculated on the plan CT, using the number of times each dose plan had been chosen. For each patient the ratio of the volume receiving 57 Gy (corresponding to 95% of the prescribed dose) for the ART strategy relative to the standard is calculated.

Results: The adaptive strategies resulted in a significant reduction of the volumes receiving a given dose, as compared with the standard RT approach. For patients with SIB the mean ratio of the volume receiving 57 Gy for method A, B and C is 0.68 (SD: 0.08), 0.70 (SD: 0.12) and 0.72 (SD: 0.16) respectively. For patients treated to the bladder only the corresponding mean ratio for the methods A, B and C is 0.61, 0.61 and 0.57 respectively.

Conclusion: Using either of the ART strategies it is possible to reduce the volumes receiving high doses significantly compared with the use of a standard non-adaptive plan. The differences in dose volume parameters between the three methods are small compared with the differences from the standard plan, in the present setting based on bony anatomy match.

Friday May 28, 2010

Marianne Knap, Aarhus, Denmark

Daily cone-beam computed tomography used to determine tumour shrinkage in lung cancer patients

M Knap[1], L Hoffmann[2], M Nordsmark[1], A Vestergaard[2]. *[1]Aarhus University Hospital, Department of Oncology, Aarhus, Denmark. [2]Aarhus University Hospital, Department of Medical Physics, Aarhus, Denmark.*

Introduction: Locally advanced non-small-cell lung cancer (NSCLC) and small-cell lung cancer (SCLC) can be cured with chemo-radiotherapy. However, the treatment volumes are usually large resulting in high risk of toxicity. During radiotherapy (RT), the lung tumour may shrink, making it possible to decrease the target volume and thereby reduce the risk of toxicity. The purpose of this study was to determine tumour shrinkage during a RT course using cone-beam computed tomography (CBTC).

Materials and Methods: From November 2009 to Marts 2010, 20 consecutive lung cancer patients (14 NSCLC, 6 SCLC) were followed with daily CBCT during RT. All 14 NSCLC patients were treated with 60-66 Gy in 30-33 fractions (F), 5F/week. Four SCLC patients were treated with 45 Gy in 30 F, 10 F/week and 2 SCLC patients were treated 50 Gy in 25 F, 5 F/week. The median time interval from the planning CT until start of RT was 14 days (range 9-20).
The gross tumour volume for lung tumour (GTV-t) was visible in all daily CBCT scans and was delineated at the beginning, halfway, and at the end of treatment. Whenever visible, the gross tumour volume for lymph nodes (GTV-n) was also delineated. The GTV-t and GTV-n volumes were determined.

Results: In 6 NSCLC patients, we observed a significant GTV-t shrinkage (15 % - 35 % from the planning CT until the last CBCT). In 3 NSCLC patients minor shrinkage (5 % - 15 %) was observed, and in 3 NSCLC patients there was no change in tumour volume. Only 2 patients presented a significant shrinkage (13 - 23 %) in the GTV-n. No tumour or lymph node growth was observed. In one SCLC patient there was a significant shrinkage in GTV-t and GTV-n (approx 30 %) and in two SCLC patients minor shrinkage was observed in GTV-t. Three patients showed no tumour or node shrinkage.

Conclusion: Approximately one third of all patients with lung cancer undergoing chemo-RT achieved significant tumour shrinkage from planning CT until the end of the radiotherapy. Daily CBCT makes it possible to select patients who will benefit from individualized adaptive radiotherapy.

Friday May 28, 2010

Sune Kristian Buhl, Herlev, Denmark

Clinical evaluation of 3D/3D MRI-CBCT automatching on brain tumors for online patient setup verification – A step towards MRI-based planning

Buhl S. K.[1], Duun-Christensen A. K.[2], Kristensen B. H.[1] and Behrens C. F.[1] *1) Department of Oncology, Copenhagen University Hospital, DK-2730 Herlev, Denmark. 2) Department of Informatics and Mathematical Modelling, Technical University of Denmark, DK-2800 Kgs. Lyngby, Denmark.*

Introduction: Magnetic Resonance Imaging (MRI) is used more and more often in modern day radiotherapy (RT) due to better soft tissue contrast. However, treatment planning based solely on MRI is restricted due to two facts: 1) Dose calculation algorithms used in RT planning uses the tissue electron density acquired from a Computer Tomography (CT) scan to asses tissue dose and 2) online patient setup verification is done by using either Digital Reconstructed Radiographs (DRR's) from a CT scan, or a CT scan itself as reference. The issue concerning tissue electron density and dose calculation has been address in a previous study. Hence, the purpose of this study is to evaluate the use of 3D/3D MR-CBCT image matching for online verification of patient setup in RT.

Materials and methods: To be able to determine the accuracy of the MRI-CBCT automatching and to perform preliminary tests of the software without involving patients, a stable multi-modality phantom was constructed using primarily polyurethane. MR and CT images of the phantom were acquired and subsequent matched with CBCT images acquired using the on-board imager (OBI) on a VARIAN Clinac iX 2100. External markings on the phantom box were used to ensure correct setup, thereby minimizing random setup errors. Automatching was performed using the OBI's software, currently based on a mutual information algorithm. Phantom results were complemented by completing 18 MRT-CBCT and CT-CBCT automatches on 3 patients undergoing RT for brain tumors.

Results: The absolute difference in couch shift coordinates acquired from automatching of MRI-CBCT and CT-CBCT, were ≤ 2 mm in the vertical direction and ≤ 3 mm in the longitudinal and lateral directions. For couch rotation, differences up to 3.3 degrees were observed. Mean values and standard deviations were 0.8 ± 0.6 mm, 1.5 ± 1.2 mm and 1.2 ± 1.2 mm for the vertical, longitudinal and lateral directions, respectively and 1.95 ± 1.12 degrees for the rotation (n = 17).

Conclusions: The use of automatic 3D/3D MRI-CBCT matching as a verification of patient setup in RT on brain tumors is possible. The results from this preliminary study show, that the difference between MRI-CBCT and CT-CBCT matching is minute. Future work includes further clinical studies on a larger patient population and a wider range of patient groups.

Friday May 28, 2010

Per Ruggaard Poulsen, Aarhus, Denmark

Dynamic MLC tracking of moving targets with a single kV imager for static field treatments

Poulsen PR[1], Cho B[2], Sawant A[3], Ruan D[3] and Keall PJ[3]. *[1]Department of Oncology, Aarhus University, Denmark. [2]Department of Radiation Oncology, Asan Medical Center, Seoul, Korea. [3]Department of Radiation Oncology, Stanford University, Stanford, USA.*

Introduction: Tumor motion during radiotherapy is a major challenge for accurate dose delivery, in particular for hypofractionation and dose painting. The motion may be compensated by dynamic MLC (DMLC) tracking. Previous work has demonstrated that a single kV imager can accurately localize moving targets for DMLC tracking during rotational delivery, however this method has not been investigated for static field geometry used for conformal and IMRT treatments. Here we investigate single kV-imager based DMLC tracking for static fields.

Materials and methods: A 5-field treatment plan with circular field shape and 200 MU per field was delivered in 20 s per field to a moving phantom with an embedded marker. Fluoroscopic kV images were acquired at 5 Hz perpendicular to the treatment beam axis during a 120° pre-treatment gantry rotation, during treatment delivery, and during inter-field gantry rotations. The 3D marker position was estimated from the kV images and used for MLC adaptation. Experiments included 12 thoracic/abdominal tumor trajectories and 5 prostate trajectories selected from databases with 160 and 536 trajectories, respectively. The tracking error was determined as the mismatch between the marker position and the MLC aperture center in portal images. Simulations extended the study to all trajectories in the databases and to treatments with prolonged duration of 60 s per field.

Results: In the experiments, the mean 2D root-mean-square tracking error (RMSE) was 1.5 mm for thoracic/abdominal tumor trajectories and 0.8mm for prostate. Simulations agreed with this to within 0.1 mm. Simulations of all trajectories in the databases resulted in mean 2D RMSE of 1.2 mm (thorax/abdomen) and 0.4 mm (prostate) for both 20s and 60s per field.

Conclusions: Single-imager DMLC tracking, which is fully compatible with IMRT, was demonstrated for static fields. The accuracy was better than 1 mm for most prostate trajectories and 2 mm for most tumor trajectories with respiratory motions.

Friday May 28, 2010

Session 8: Particle therapy

Håkan Nyström, Uppsala, Sweden

The role of Protons in Biologically-Guided Adaptive Radiotherapy

Nyström H, *The Skandion Clinic, Uppsala, Sweden.*

With the introduction of new biologically based imaging possibilities, a higher degree of individualisation and adaptation of radiotherapy will be possible. Better knowledge of the biology of the target and its sub-volumes will enable dose prescriptions tailored to the individual patients, tissues and sub-volumes. Repeated imaging during the course of treatment will in addition enable adaptation of the treatment to cope with anatomical, as well as biological changes of the patient and of the target tissues.

To bring these bright future perspectives into an equally bright improvement of clinical outcome, advanced tools to tailor the physical dose distributions are needed. The most conformal radiotherapy technique known to mankind and clinically available today is proton therapy; in particular Intensity Modulated Proton Therapy (IMPT) with active spot scanning can not only tailor the dose to the desired target, but also effectively avoid sensitive structures in the proximity of the target to a degree far better than other conformal techniques such as IMRT.

The development of IMPT is now mature enough for clinical introduction on a broader scale. Economically proton therapy is still less affordable than conventional radiotherapy, but with the present rapid increase in the number of proton facilities world wide and new initiatives to improve efficiency, the difference in affordability will continue to decrease and in comparison with the benefits, soon even further diminish.

Contrary to what is sometimes claimed, the demands for better physical dose distributions and better avoidance of non-target tissue, has never been higher. Prolonged expected survival in many groups of patients enhances the strive for reduction of late toxicities and the success of concomitant systemic therapies, with their tendency of adding higher morbidity, even further stresses the increased need for subtle dose sculpturing tools.

There is no contradiction in the endeavour for better physical dose distributions and a more biologically based approach. On the contrary, physical dose distributions are the tool to which achieve a treatment that can meet the biological demands.

Friday May 28, 2010

Stephanie E. Combs, Heidelberg, Germany

Heidelberg Ion Therapy Center (HIT): The First 80 Patients

Stephanie E. Combs[1], Malte Ellerbrock[2], Thomas Haberer[2], Daniel Habermehl[1], Angelika Hoess[2], Oliver Jäkel[2,3], Alexandra Jensen[1], Swantje Klemm[2], Marc Münter[1], Jakob Naumann[2], Anna Nikoghosyan[1], Susanne Oertel[1], Katia Parodi[2], Stefan Rieken[1] and Jürgen Debus[1]. *1) University Hospital of Heidelberg, Department of Radiation Oncology, Im Neuenheimer Feld 400, 69120 Heidelberg, Germany. 2) Heidelberger Ionenstrahl Therapiezentrum (HIT), Im Neuenheimer Feld 450, 69120 Heidelberg, Germany. 3) German Cancer Research Center (DKFZ) Heidelberg, Dep Medical Physics in Radiation Oncology, Im Neuenheimer Feld 280, 69120 Heidelberg, Germany.*

Introduction: The Heidelberg Ion Therapy Center (HIT) started clinical operation in November 2009. In this report we present the first 80 patients treated with proton and carbon ion radiotherapy and describe patient selection, treatment planning and daily treatment for different indications.

Materials and Methods: Between November 15th, 2009 and April 15th, 2010, 80 patients were treated at the Heidelberg Ion Therapy Center (HIT) with carbon ion and proton radiotherapy. Main treated indications consisted of skull base chordoma (n=9) and chondrosarcoma (n=18), malignant salivary gland tumors (n=29), chordomas of the sacrum (n=5), low grade glioma (n=3), primary and recurrent malignant astrocytoma and glioblastoma (n=7) and well as osteosarcoma (n=3). Of these patients, 4 pediatric patients aged under 18 years were treated.

Results: All patients were treated using the intensity-modulated rasterscanning technique. 76 patients were treated with carbon ions (95%), and four patients were treated with protons. In all patients X-ray imaging was performed prior to each fraction. Treatment concepts were based on the initial experiences with carbon ion therapy at the Gesellschaft für Schwerionenforschung (GSI) including carbon-only treatments and carbon-boost treatments with photon-IMRT. The average time per fraction in the treatment room per patient was 29 minutes; for irradiation only, the mean time including all patients was 16 minutes. Position verification was performed prior to every treatment fraction with orthogonal X-ray imaging.

Conclusion: Particle therapy could be successfully included into the clinical routine at the Department of Radiation Oncology in Heidelberg. Numerous clinical trials will subsequently be initiated to precisely define the role of proton and carbon ion radiotherapy in radiation oncology.

Friday May 28, 2010

Per Munck af Rosenschöld, Copenhagen, Denmark

On-line adaptive intensity modulated proton therapy of lung cancer – a treatment planning study of 2D tracking

Munck af Rosenschöld P1, Aznar MC1, Nygaard DE1, Persson GF1, Korreman SS1,2, Engelholm SA1, Nyström H3. *1. Department of Radiation Oncology, Copenhagen University Hospital (Rigshospitalet), Copenhagen, Denmark. 2. Department of Human Oncology, University of Wisconsin-Madison, Madison, USA. 3. The Skandion Clinic, Uppsala, Sweden.*

Purpose: To study the robustness intensity modulated (spot-scanned) proton therapy (IMPT) with respect to target dose coverage, and to evaluate the possible improvement of performing a simplistic adaptive therapy using on-line two-dimensional (2D) lung tumour tracking.

Methods: Four-dimensional (4D) CT scans were collected under free breathing for patients with early stage or locally advanced lung cancer. Five consecutive patients with a three-dimensional tumour displacement of 0.3-2.4 cm were selected for this study. IMPT plans to 45 Gy in 3 fractions were made using the EclipseTM treatment planning system (Varian Medical Systems, USA), using a co-planar 3-field technique. The plans were made on the midventillation bin and then recalculated on each of the 10 bins of the 4DCT. One additional set of plans were made where the beam was moved to accommodate for tumour displacement. The total absorbed dose was summed to the midventilation bin based on deformable image registration (VelocityAITM, Velocity Medical Solutions, USA).

Results: Around 97-100% of the gross tumour volume (GTV) was covered by 95% of the prescribed dose (V95) for a tumour displacements of less than 1 cm. Tumour tracking provided no or only minor improvement for 4 out of 5 patients on the GTV dose coverage. For these 4 patients, typically two to three bins of the 4DCT demonstrated rather poor dose coverage of the GTV, but the summed dose distribution proved to be fairly robust. However, for the patient with the large tumour displacement of 2.4 cm, the tracking provided a markedly improved dose coverage with a V95 of 97% vs. 52% to the GTV with and without tracking, respectively. The interplay effect of the scanning of the proton beam and the tumour motion was disregarded in the present study.

Conclusion: The 3-field technique employed in the present study proved to result in V95 of around 97-100% for the GTV for tumour displacements of less than 1 cm with or without 2D tumour tracking, which was 4 of out the 5 patients studied. Interestingly, the 2D tumour tracking method provided an adequate target coverage for the patient with a large tumour displacement of about 2 cm, suggesting that on-line adaptation of the proton energies recommended previously [1] may be redundant. Further studies are required to clarify if IMPT and 2D tracking of lung cancer is a viable treatment strategy compared to other effective methods [1,2].

1. Engelsman M, Rietzel E, Kooy HM. Four-dimensional proton treatment planning for lung tumors. Int J Radiat Oncol Biol Phys 2006;64:1589 –1595.

2. Kang Y, Zhang X, Chang JY, Wang H, Wei X, Liao Z, Komaki R, Cox JD, Balter PA, Liu H, Zhu XR, Mohan R, Dong L. 4D Proton treatment planning strategy for mobile lung tumors. Int J Radiat Oncol Biol Phys. 2007 Mar 1;67(3):906-14.

Friday May 28, 2010

Niels Bassler, Aarhus, Denmark

Dose- and LET-painting with particle therapy

Niels Bassler, Oliver Jäkel, Christian Skov Søndergaard and Jørgen BB Petersen.

Background: Tumour hypoxia has been identified as being one of the limiting factors in obtaining tumour control in radiotherapy for some tumours. The additional dose needed in order to overcome hypoxia is expressed by the Oxygen Enhancement Ratio (OER). A simple strategy is then to escalate the dose to the tumor, which is, however, limited by the risk of normal tissue complication. A more sophisticated strategy is to identify the hypoxic compartments of a tumour by functional imaging parameters and perform "dose painting" as a function of a hypoxic signal. A different strategy is to use high LET radiation, such as carbon ions. These have been shown in in-vitro experiments to exhibit a reduced OER. The high-LET region of a beam of heavy charged particles such as carbon ions is located in the distal part of the Bragg peak. A modulated or "spread out" Bragg peak is a weighted function of several Bragg peaks at various energies, which however results in a dilution of the dose-average LET in the target volume. Here, we investigate the possibility to redistribute the LET by dedicated treatment plan optimization, in order to maximize LET in the target volume. This may be a strategy to potentially overcome hypoxia along with dose escalation or dose painting.

Materials and Methods: By using the carbon ion and proton treatment planning system TRiP in conjunction with a custom in-house developed software package "pytrip", we have investigated the dose-average LET as a function of PTV volume for simple configurations in a first step. In the next step, the dose averaged LET for a fixed volume was investigated as a function of depth in water. Finally, mixed modality treatment plans using protons and carbon ions are optimized in order to investigate, how the high-LET region can be shaped nearly arbitrarily throughout the PTV, which we call LET-painting.

Results: By reduction of the PTV size of carbon ion fields, the dose average LET is significantly increased, and can be more effectively used as a "LET boost" on hypoxic tumour compartments. The dose-average LET though does not depend strongly on the depth of the PTV. The high-LET region can be shaped in very different ways, while maintaining the distribution of the absorbed dose or biological effective dose. Treatment plans involving only carbon ion beams, show very different LET distributions depending on how the fields are arranged. Also for mixed radiation modalities, significant "LET boosts" can be achieved at nearly arbitrary positions within the target volume.

Conclusion: We demonstrate that the LET distribution is an additional parameter in treatment planning for particle beams, which can be optimized. An LET boost can also be applied in multimodal treatment planning, such as combining carbon ions with protons and/or photons. Following the general understanding of the relationship between hypoxia, LET and OER, we conclude, that an additional therapeutic advantage can be achieved by confining the high-LET part of the radiation in hypoxic compartments of the tumour, and applying low-LET radiation to the normoxic tissue. We also anticipate that additional advantages may be achieved by deliberate sparing of normal tissue from high LET regions. Consequently, treatment planning based on simultaneous dose and LET optimization has a potential to achieve higher tumour control and/or reduced NTCP.

POSTERS

Daily kV cone-beam CT and deformable image registration as a method for studying dosimetric consequences of anatomic changes in adaptive IMRT of head and neck cancer

Ulrik Vindelev Elstrøm[1,2], Barbara Anna Wysocka[1], Ludvig Paul Muren[1,2], Jørgen BB Petersen[2], Cai Grau[1]. *[1]Department of Oncology, Aarhus University Hospital, Aarhus, Denmark. [2]Department of Medical Physics, Aarhus University Hospital, Aarhus, Denmark.*

Purpose: To propose and test a method for assessment of anatomic changes and actually delivered doses during radiotherapy (RT) of head and neck cancer utilizing volumetric images from cone-beam CT (CBCT) and a commercially available deformable image registration (DIR) software.

Methods and Materials: Thirty-three CBCT image sets acquired during daily image-guided RT of one head and neck cancer patient were retrospectively transferred from a standard treatment planning system (TPS) to the DIR software, along with the planning CT. Each CBCT worked as a template for deformation of the planning CT followed by propagation of contours delineated for the planning purpose. The problem of deteriorate Hounsfield unit values in CBCT-based dose calculation was avoided by transfer of each deformed planning CT back into the TPS. Based on these, a re-calculation of the actual delivered dose distribution on a daily basis was performed, also taking the contribution from online image-guidance into account. Dose-volume histogram (DVH) parameters were calculated at each treatment fraction. The method was evaluated for time consumption and the deformed contours were evaluated clinically by assessing the concordance with anatomical position and shape of the corresponding structures on CBCT.

Results: For the patient case studied, the workflow of the method took 45 minutes (median; range 30-67 min.) to estimate the delivered dose for each treatment fraction. There was no statistically significant time trend throughout the treatment fractions (p=0.42). The evaluation of propagated deformed contours scored for normal tissues (165 structures in total) good (contour accurate) for 32.5% and acceptable (minor inconsistencies) for 77.5%. The target volumes (99 structures) were similarly scored as satisfactory representatives for the purpose of extracting DVH parameters. Based on daily DVH parameters the actual delivered dose could be monitored throughout the treatment course. The dosimetric effect of 7% relative weight loss was clearly observed and the potential for dose reduction in normal-tissue structures such as the parotid glands (10% overdosed) by adaptation of the treatment plan was disclosed.

Conclusion: A proof-of-principle method to quantitatively monitor changes in anatomy and delivered dose during the course of fractionated RT for H&N cancer has been demonstrated. This provides a tool for development of adaptive strategies for re-planning head and neck cancer patients with respect to action thresholds, timing and frequency.

Investigation of respiration induced intra- and inter-fractional tumour motion using a standard Elekta Cone Beam CT

Karina Lindberg Gottlieb, Ph.D.1, Christian Rønn Hansen, M.S.1, Olfred Hansen, M.D., Ph.D.2 and Carsten Brink, Ph.D.1,3. *1 Laboratory of Radiation Physics, Odense University Hospital, Odense, Denmark. 2 Department of Oncology, Odense University Hospital, Odense, Denmark. 3 Faculty of Health Sciences, University of Southern Denmark, Odense, Denmark.*

Introduction: The main purpose of this study is to investigate whether a standard cone beam CT (CBCT) scan can be used to determine the intra-fractional tumour motion for lung tumours that also has infiltrated the mediastinum. If it is possible to time resolve a standard CBCT acquired before the treatment, it can be used to verify the size of the intra-fractional tumour motion during the treatment course and investigate whether the respiration induced motion for lung tumours with mediastinal infiltration changes during the treatment course (from planning CT till late in the treatment course).

Material and Methods: This study includes 23 patients with NSCLC. Analysis of the intra-fractional tumour motion has been performed for each patient on a 4D-CT scan as well as on 3 4D-CBCT (fractions 3, 10 and 20). The delineation of the tumour (GTV) has been performed on the first phase of the 4D-CT. Registration of phase one from the 4D-CT and 4D-CBCT was used to transfer the GTV to the CBCT scans. Hereafter the motion of the outlined GTV was tracked in the planning 4D-CT and the 3 4D-CBCT using Pinnacle3™ version 8.1w (research version). Additionally, the inter-fractional tumour movement (relative to the bony structure) was obtained from the difference in tumour position between the mid-ventilation phase of the 4D-CT and the 3D-CBCT.

Results: It has been possible to track lung tumour with mediastinal infiltration in the 4D-CBCT scan based on a standard 3D-CBCT. A paired t-test shows that the respiration motion in the 4D-CBCT is not significantly different from the result found from the initial 4D-CT. Likewise, no differences in respiration motion was found between fractions 3, 10 and 20. The standard deviation of the respiration induced tumour motion based on all 4D-CT and 4D-CBCT scans was measured to be: Intra: 0.7 mm (LR), 1.0 mm (AP), 1.8 mm (CC) and Inter: 1.4 mm (LR), 1.5 mm (AP), 1.5 mm (CC).

Conclusion: This study shows that it is possible to track tumour motion for NSCLC patients with mediastinal infiltration using standard CBCT data available in all institutions using Elekta CBCT. No clinically relevant change in the intra-fractional tumour motion was observed during the fractionated treatment course. Thus, it has been shown that the tumour motion measured from the 4D-CT is representative of the tumour motion during the entire treatment.

A novel mathematical model for the radiobiological evaluation of an adaptive course of treatment

Francisco Cutanda Henríquez (1) and Silvia Vargas Castrillón (2). *(1) Servicio de Medicina Nuclear. Hospital General Universitario Gregorio Marañón. Calle Doctor Esquerdo, 46. 28007. MADRID (Spain). (2) Laboratorio de Metrología de Radiaciones Ionizantes. CIEMAT. Avda. Complutense, 22. 28040. MADRID (Spain).*

Introduction: The adaptation of treatment parameters to fit changes in patient anatomy causes that the original dose distribution does not contain enough information to predict or, at least, to estimate tumor control probability. A novel method is described that allows a fully customized modeling of the distribution of clonogens after n irradiations and p pauses.

Methods: Clonogen distribution is treated as a probability problem, and the transition of the distribution after the j-eth treatment fraction can be obtained from the j-1-eth distribution via a suitable operator, depending, among other parameters, on the dose distribution within the PTV.

Results: Two examples of application of this method are provided as an illustration. Furthermore, a check on consistency is shown to give positive results.

Conclusions: The method presented here involves a great number of operations, but it has two advantages: it is adaptable to any survival function, and it provides the complete probability distribution of surviving clonogens at any stage in the treatment, taking into account to any minor adaptation.

Investigation of the dosimetric impact of a Ni-Ti fiducial marker in carbon and proton beams

Herrmann R.1,2, Carl J.3, Jäkel, O.4,5, Bassler, N.1,2, Petersen J. B. B.6. *1) Dept. of Physics and Astronomy, Aarhus University, Denmark. 2) Dept. of Exp. Clinical Oncology, Aarhus University Hospital, Denmark. 3) Dept. of Med. Physics, Oncology, Aalborg Hospital, Denmark. 4) Heidelberg Ion Beam Therapy Center, Germany. 5) German Cancer Research Center Heidelberg, Germany. 6) Dept. of Med. Physics, Aarhus University Hospital, Denmark.*

Introduction: Fiducial markers based on a removal stent are currently used in image guided radiotherapy. Here it is investigated what the possible dosimetric impact of such a marker could be, if used in proton or carbon ion treatment, by using Monte Carlo simulations.

Methods: The simulations have been done using the Monte Carlo particle transport code FLUKA the default hadron therapy settings. A 3 cm long stent is approximated in FLUKA by stacking hollow tori. To simulate realistic clinical conditions a field 5 x 5 cm has been used, deliveringa 5 cm wide spread out Bragg peak located 5 cm deep for protons and carbon ions. The stent has been arranged perpendicular, turned 45 degrees, and parallel to the beam axis. Depth-dose profiles have been simulated and the LET directly behind the stent were calculated.

Results: The position of the 95% dose level shifts for carbon ions 5 mm into negative beam direction for the marker perpendicular to the beam and 7 mm if the stent is turned 45 degree for a 1 x 1 cm dose binning on the center beam axis. For the case where the stent parallel to beam direction the 95% dose level shifts 26 mm. For protons, the shift of the 95% dose level is less, due to the increased scattering compared to carbon ions. The shift for a perpendicular arranged marker is 4 mm, for 45 degrees turned it is 6 mm. For the case where the stent was oriented parallel to the beam, the observed shift is 18 mm. Dose inhomogeneities caused by straggling effects occur only near the distal
edge of the field.

Conclusions: The dose average LET increases directly behind the marker up to 10 % for carbon ions as well as for protons. The results of our investigations show that the Ni-Ti marker has a non negligible impact on the dose distributions for the used radiation types. However if the treatment plan rules out narrow angles between symmetry axis of the stent and the beam direction, this may be compensated.

Neutron Fluence in Antiproton Radiotherapy - Measurements and Simulations

Bassler, N [1,2], Holzscheiter, M. H. [3,4], Petersen, J. B. B. [5]. *1. Dept. of Physics and Astronomy, University of Aarhus, Aarhus, Denmark. 2. Dept. of Experimental Clinical Oncology, University Hospital, Aarhus, Denmark. 3. Dept. of Physics & Astronomy, University of New Mexico, Albuquerque, USA. 4. Max Planck Institute for Nuclear Physics, Heidelberg, Germany. 5. Department of Medical Physics, University Hospital, Aarhus, Denmark.*

Introduction: Antiprotons are studied as possible candidates for particle beam cancer therapy because of enhanced dose deposition at end of range due to annihilation. A significant part of the secondary particle spectrum from antiproton annihilation consists of fast neutrons, which may contribute to a significant dose background found outside the primary beam and could lead to an elevated risk of secondary cancer.

Material & Methods: Using Lithium-6 and -7 Fluoride TLD pairs and a polystyrene phantom as a moderator, we have performed absolute fluence measurements of the part of the fast neutron spectrum thermalized in the target.

Results: The experimental results are found to be in good agreement with simulations using the Monte Carlo particle transport code FLUKA. We find a low contribution from thermal neutrons, however the substantial amounts of fast neutrons may restrict antiproton therapy to smaller target volumes. These results are found to be similar to values calculated for pion treatment, however exact modeling under more realistic treatment scenarios is still required to quantitatively compare these findings to those for other treatment modalities.

Cone-Beam CT for setup of patients with Cancer in the Cervix Uterus: Comparing 3D match with 6D match on the whole body as well as soft tissue.

Jakobsen, K.L. Christensen, B.H. Sjöström, D.P.F. *Copenhagen University hospital, Herlev, Department of Oncology (R), Division of Radiophysics (51AA), Herlev Ringvej 75, DK-2730 Herlev.*

Introduction: Delivering a high dose to the tumor but sparring the normal tissue is crucial in radiotherapy. Over the last decade new modalities of imaging has been developed. Therefore it is now possible to follow even the tumor-position during the course of treatment.The aim of this study was to analyze the influence of the three rotations on the size of the three translations needed to reposition the patient. Further, the aim was to analyze the rotational influence on the dose distribution especially in the elective target furthest from the isocenter.

Materials and methods: Our institution is equipped with 8 Varian™ iX accelerators with On-Board Imaging device used for orthogonal images as well as ConeBamCT (CBCT). The orthogonal images were acquired every day and the patient repositioned CBCT were acquired once a week. All images were analyzed in "Offline Review (8.9)".The patients suffered from Cancer in the Cervix Uterus. The data analyzed was the difference between the CBCT and the orthogonal images. The CBCT match on soft tissue with 3 Degree Of Freedom (DOF) was compared to the same match with 6 DOF. The same comparison was made for the match on the whole body. For dosimetric evaluation the CBCT were analyzed in "Eclipse 8.9" with an overlay of dose from the planning CT.

Results: The difference between match done with 3 DOF and 6 DOF is very small (2 mm in mean). The rotations are small as well (a maximum of 5°).The vessels used to define the elective CTV can be seen on the CBCT too and the translation for this area also seems small (2-3 mm).

Conclusion: Utilizing the CBCT it is possible to quantify the impact of rotation on the necessary translations. For the data collected to date the influence has been small but so has the rotations.The analysis of the dosimetric data indicates that it may be possible to shrink the CTV to PTV margin for the elective volumes. Before this can be done safely, it must be ensured that the GTV to CTV margin is of the correct size.

Feasibility and Sensitivity Study of Helical Tomotherapy for Dose Painting Plans

Deveau MA[1], Bowen S[1], Westerly D[2], Jeraj R[1] *(1) Department of Medical Physics, University of Wisconsin - Madison, Madison, WI, USA (2) University of Colorado - Denver, Aurora, CO, USA.*

Purpose: Important limitations for dose painting are due to treatment planning and delivery constraints. The purpose of this study was to develop a methodology for creating voxel-based dose painting plans that are clinically deliverable using the clinical TomoTherapy Hi-Art II (TomoTherapy Inc, Madison, WI) treatment planning system (TPS).

Methods and Materials: Uptake data from a head and neck patient who underwent a [^{61}Cu]Cu-ATSM (hypoxia surrogate) PET/CT scan was retrospectively extracted for planning. Non-uniform voxel-based prescriptions were converted to structured-based prescriptions for compatibility with the Hi-Art II TPS. Optimized plans were generated from permutations of physical objectives for each prescription sub-volume, which included variable structure importance, prescription point normalization, iteration number, DVH volume, Min/Max dose, and dose penalty. Delivery parameters such as pitch, jaw width and modulation factor were also varied. Avoidance structures were constrained to clinical tolerances. The PTV volume receiving planned dose within 5 percent of the prescription ($Q_{0.95\text{-}1.05}$) was used to evaluate plan conformity.

Results: Plan conformity decreased as the integral boost doses increased from 10 Gy to 30 Gy ($Q_{0.95\text{-}1.05}$: 97% vs 78%) and as the prescription DVH constraint ($Q_{0.95\text{-}1.05}$: 88% vs. 84%) or the normalization point ($Q_{0.95\text{-}1.05}$: 88% vs. 85%) deviated from the means. The conformity increased for decreasing jaw width from 5.0 cm to 1.05 cm ($Q_{0.95\text{-}1.05}$: 68% vs 87%), modulation factors greater than 1.0 ($Q_{0.95\text{-}1.05}$: 35% vs 86%), and increasing iteration number from 100 to 1000 ($Q_{0.95\text{-}1.05}$: 80% vs 86%). Delivery times ranged from 4 to 22 minutes for changes in field width, pitch (0.860 to 0.172), or modulation factor (1 to 4).

Conclusions: This investigation demonstrated the ability of the Hi-Art II TPS to create voxel-based dose painting plans. Results indicated that agreement in prescription dose and planned dose distributions for all plans were sensitive to physical delivery parameter changes in jaw width and modulation factors greater than 1.5, but insensitive to changes in pitch. Tight constraints on target structures also resulted in decreased plan conformity while under a relaxed set of optimization parameters, plan conformity was increased.

Uncertainty of textural features in PET images due to different acquisition mode and reconstruction parameters.

Galavis P[a], Hollensen C[b,c], Paliwal B[a], Jeraj R[a]. *[a] Dep. of Medical Physics, University of Wisconsin, Madison, USA. [b] Dep. of Informatics and Mathematical Models, Techn. University of Denmark, Copenhagen, Denmark. [c] Dep. of Radiation. Oncology, Copenhagen University Hospital-Rigshospitalet, Denmark.*

Purpose: Characterization of textural features, spatial distributions of image intensity levels, has been considered as a tool for automatic tumor segmentation. This work studies the uncertainties of the textural features in PET images due to different acquisition and reconstruction parameters.

Methods and Materials: Fifteen patients with solid tumors underwent PET/CT on a GE Discovery VCT scanner, 60-90 minutes post-injection of 10mCi of [^{18}F]-FDG. Scans were acquired in both 2D and 3D mode. For each acquisition the raw PET data was reconstructed within clinical setting, by varying grid size, post-reconstruction filter width and the number of iterations in the reconstruction algorithm. Lesions were segmented on a default image using thresholds of 40% of maximum SUV. The obtained contour was superimposed on the other nine sets of images. 50 different texture features, such as first order (entropy, energy) and second order (homogeneity, contrast and coarseness) were calculated inside the tumors. For second order calculations, the SUV was linearly scaled to 256 grey levels and the gray-tone-spatial dependence matrices were used. Maximum and minimum variations of the features were calculated with respect to the default image.

Results: Varying acquisition and reconstruction parameters caused small changes for some features such as, energy and entropy while for other such as homogeneity, contrast and coarseness large changes were observed. The uncertainty ranges were between -1% to 1% for the entropy, -2% to 2% for the energy, while ranging from -5% to 60% for homogeneity, from -130% to 15% for contrast, and from -15% to 65% for coarseness.

Conclusion: Textural features such as the entropy and energy were found to be less sensitive to image acquisition mode and reconstruction parameters than the homogeneity, contrast and coarseness. The features with low level of uncertainty are better candidates for reproducible tumor segmentation as well as potential candidates for multi-center trials focusing in treatment assessment.

Robustness of Apparent Diffusion Coefficient (ADC) diffusion weighted MR imaging in cervical cancer. Dependence on B-values used.

Jesper F. Kallehauge[a], Kari Tanderup[a], Søren Haack[b], Thomas Nielsen[c], Jacob Lindegaard[a], Erik Morre Pedersen[d]. ***a*** *Department of Oncology, Aarhus University Hospital, Aarhus, Denmark.* ***b*** *Department of Biomedical Engineering, Aarhus University Hospital, Aarhus, Denmark.* ***c*** *Interdisciplinary Nanoscience Center, University of Aarhus, Denmark. Department of Radiology, Aarhus University Hospital NBG, Aarhus, Denmark.*

Background and purpose: Diffusion Weighted Magnetic Resonance Imaging (DWI) has been suggested as a noninvasive marker for tumor response in cervical cancer and may ultimately allow for individually adapted radiotherapy. The apparent diffusion coefficient (ADC) is in principle a quantitative parameter allowing for absolute comparison between patients and institutions. However, the calculated ADC value depends on the choice of diffusion gradients (quantified as so-called b-values), mainly because perfusion contributes to the signal at low b-values. It is generally agreed that by using b values larger than 150 $x10^{-3}$ s/mm^2 the ADC values will not be influenced by perfusion and will depend mono-exponentially on b-value. The purpose of this study was to determine the dependence of ADC values on the choice of low b-values.

Material and methods: The data acquisition was done using a 3T MR-scanner (Philips Achieva 3T-X) using single shot EPI based DWI in three patients with locally advanced cervical cancer prior to radiotherapy. Each scan consisted of 16 b-values (0, 10, 30, 50, 75, 100, 125, 150, 200, 400, 700, 1000, 1200, 1500, 2000, 2500) x 10^{-3} s/mm^2. Voxel size was 2.7 x 2.7 x 5 mm and total scan time was 18:30 min. The reference ADC value was calculated using a bi-exponential model In the b-value range [0,1000] x 10^{-3} s/mm^2 to take into account both perfusion and diffusion. The data processing was done using in house scripts constructed In Matlab©. The Region Of Interest (ROI) was chosen in the tumor region showing lowest ADC value in a map constructed on the basis of all the acquired b values. In order to compare common b-value schemes with the dataset that completely describes the signal curve, ADC values were calculated for 11 combinations of b-values (see table).

Results: The table shows the percentage difference between each b value scheme and the reference ADC value. The inclusion of b=0 s/mm^2 in a mono-exponential fit resulted in overestimation of ADC value by 10-48%. The most reliable schemes was using b values ≥ 150 s/mm^2 and including at least one b value ≥ 700 s/mm^2. This resulted in deviations from reference values of less than 10%. However, there is a certain bias since the reference ADC values were estimated inside the range b=[0,1000] $x10^{-3}$ s/mm^2. Using 400 s/mm^2 as upper b value resulted in significant overestimation.

Conclusions: When calculating ADC values it is imperative to understand the physical properties behind the data acquisition in order to make a correct selection of relevant b values. ADC values vary significantly depending on which b-values are used. By choosing b=150 s/mm^2 as the lower b-value the perfusion effects on ADC value are reduced. These prelimi-

nary data indicate that use of ADC value as a quantitative parameter for dose planning in radiotherapy would require that ADC values are calculated according to a common standard.

b-values [s/mm^2]	Deviation Patient 1	Deviation Patient 2	Deviation Patient 3	Average
0+400	48%	20%	45%	38%
0+700	27%	16%	27%	23%
0+1000	18%	10%	14%	14%
0+400+700	25%	14%	29%	23%
0+700+1000	18%	12%	16%	16%
150+400	23%	20%	15%	19%
150+700	10%	9%	8%	9%
150+400+700	9%	10%	8%	9%
150+700+1000	6%	5%	0%	4%
150+1000	6%	4%	-1%	3%
[150;1000]	5%	5%	1%	3%
Reference ADC [x10^{-3} mm^2/s]	0,67±0,05	0,74±0,06	0,69±0,07	

Adaptive field margin: Accounting for interfraction motion variation offers negligible effect for most patients

Korreman, S. *Department of Radiation Oncology, Rigshospitalet, Copenhagen, Denmark. Department of Human Oncology, University of Wisconsin School of Medicine and Public Health, Madison, Wisconsin, USA. Niels Bohr Institute, University of Copenhagen, Copenhagen, Denmark.*

Purpose: To investigate the magnitude of treatment field margin adaptation which can be obtained by accounting for inter-fraction changes in lung tumour motion magnitude, when all sources of uncertainty are included in margin calculations.

Methods and materials: Initial treatment field margin calculations for lung tumours including the main sources of uncertainty - target delineation error, intra- and inter-fraction target motion and setup uncertainty - were carried out according to the van Herk formula. Magnitudes of all uncertainties except intra-fraction tumour motion were taken from literature. Intra-fraction tumour motion magnitudes from 1 mm to 30 mm were simulated. Calculations were done for three different motion management strategies; no motion management, 4DCT for treatment planning and daily 4D image guidance. For each motion management strategy, inter-fraction motion magnitude variations of up to +/- 50% were simulated, and corresponding treatment field margin changes were calculated.

Results: The initial calculated field margins for the three motion management strategies for motion magnitudes 1-30 mm ranged: 15-38 mm for no motion management, 15-24 mm for 4DCT, and 8-19 mm for 4D image guidance. Simulation of motion magnitude variations yielded treatment field margin changes ranging from 0 up to 7 mm. Changes smaller than 1 mm was found for initial motion less than 10 mm for the no management strategy and the 4DCT strategy, and 9 mm for the 4D image guidance strategy. Changes smaller than 2 mm were correspondingly found for initial motion less than 14, 14 and 13 mm.

Conclusions: Using treatment field adaptation to account for inter-fraction changes in lung tumour motion magnitude yields negligible effect except for large tumour motions. A recent patient study presented at ASTRO 2009 supports the findings of the present study, showing shallow curves for treatment field margin as a function of motion magnitude. In this study, only 20% /15% of the patients exhibited motion larger than the levels for which the present study showed more than 1/2 mm potential field margin magnitude change by adaptation.
Projected TCP and NTCP implications of margin adaptation will be discussed for select patients from the mentioned study.

Investigation of breast setup accuracy using both surgical clips and patient anatomy with the EXACTRAC ® and 2D/3D ON-BOARD IMAGER ® systems

Sjöström D and Kristensen B H. *Radiotherapy, Oncology Dept., Herlev Hospital, Herlev Ringvej 75, DK-2730 Herlev, Denmark.*

Introduction: Moving towards more complex 3D treatment planning presuppose a precise treatment which requires IGRT. The setup of breast cancer patients is highly influenced by the positioning of the arms and the thorax and easy confident validation is essential. It is also important to know the limitations of the IGRT system used. This work compares on breast cancer the kV and infrared (IR) part of the ExacTrac® (ET) system with the Varian kV 2D/3D On-Board Imager® (OBI2D/OBI3D) and MV PortalVision™ (PV) systems.

Matererials and methods: 1) The IR-ET system was used with 7 spherical markers on the upper body and arms. The system detects translational and rotational rigid setup errors in 6D. 2) The kV-ET system detects setup errors in 6D by comparing two 2D kV images with multiple online generated DRRs. 3) The OBI3D cone beam CT system provides a true automated 3D/3D match. 4) For the OBI 2D system two orthogonal projections in 0/270 degrees were used. 5) MV images of the tangential treatment fields were generated with the PV system. For ten breast cancer patients the positioning of both patient anatomy and surgical clips was investigated by acquiring images with all modalities.

Results: Patient study demonstrates that adequate IR-ET positioning is verified with all other modalities when anatomy landmarks were used. When the IR-ET system indicated a mismatch the kV-ET, OBI3D and the PV systems revealed that the positioning of the patient was deprived. All modalities demonstrates high patient setup precision (< 3 mm and < 1 degree) when anatomy landmarks were used. Furthermore the comparison demonstrates that all modalities agree with OBI3D within a mean of 3 mm and 1.1 degree. In general similar results were found when matching on the surgical clips. However, for some of the patients it was not possible to identify all clips leading to misinterpretation of the match. This was particular hard to identify on the IR-kV system because of the special oblique geometrical configuration of the x-ray image system.

Conclusions: Only the ET and the OBI3D directly identifies and quantifies pitch and roll rotations which are particularly important for tangential field techniques. However, automatic matching with the kV-ET system can lead to misalignment caused by misinterpretation of the images e.g. when non-rigid deformation exists. The use of surgical clips together with e.g. ET-kV could be of interest for partial breast treatment.

Changes in target delineation for high grade glioma using 18 FDG PET fused with MRI and CT.

Lassen-Ramshad Y*, Pilloy W, Untereiner M***.** **Oncological Department, Aarhus Universityhospital, Danmark, **National PET Centre Luxembourg, Luxembourg, ***National Radiotherapy Centre Centre Francois Baclesse, Esch/Alzette, Luxembourg.*

Introduction: Since the introduction of the concomitant treatment with radiotherapy and chemotherapy with Temozolomide for high grade malignant glioma patients benefit from longer survival. But still their disease is unfortunately in most cases fatal and the disease almost always recurs in the radiation treatment field. Target definition for radiotherapy is usually done with the doseplanning CT scan, sometimes also with image fusion with the patient's MR scans. Using PET scans for target delineation could facilitate the identification of the biological active part of the disease, by this offering us a better target delineation.

Methods: Since 2002 patients treated for high grade glioma at the national radiotherapy centre in Luxembourg had a postoperative FDG PET scan that was fused with the patients MRI scans and the treatmentplanning CTscan for target delineation. We performed a volumetric study for 29 patients comparing the treatment volumes defined with and without FDG PET for each patient.

Results: The gross tumor volume defined with PET was different from the GTV defined with MRI or the GTV defined with the treatment planning CT alone. In average 30% of the PET volume was not defined with the CT and in average 41% of the PET volume was not defined with the MRI.

Conclusion: We find target delineation for high grade glioma more precise using multiple image fusion that combine morphological imaging with biological imaging more precise than using the morphological imaging alone. This might also be a possibility to reduce CTV margins because of more precise volume definition and thus lowering longterm treatment toxicity. Future studies maybe with other tracers or comparisions with MRI spectroscopy could be interesting.

Residual rotational set-up errors after daily cone-beam CT image guidance in locally advanced cervical cancer.

Louise Vagner Laursen, Ludvig Muren, Ulrik Vindelev Elstrøm, Anne Vestergaard, Jacob Lindegaard, Cai Grau, Kari Tanderup. *Department of Oncology, Aarhus University Hospital, Norrebrogade 44 bldg. 5, 8000 Aarhus C, Denmark. Department of Medical Physics, Aarhus University Hospital, Norrebrogade 44 bldg. 5, 8000 Aarhus C, Denmark. Institute of Clinical Medicine, Aarhus University, Brendstrupgaardsvej 100, 8200 Aarhus N, Denmark.*

Background: Through the application of daily image guidance in radiotherapy (RT) it is possible to correct for translational set-up errors whereas residual rotational errors cannot be corrected for with a conventional couch. In particular pitch and yaw errors can result in target displacements which increase with distance from the treatment isocenter. The purpose of this study is to evaluate the residual rotational component of set-up errors by the use of daily kilovoltage cone-beam CT (CBCT) in cervical cancer patients.

Methods and Materials: A total of 25 locally advanced cervical cancer patients (650 CBCT scans in total) were studied. Patients were treated with 45-50 Gy in 25-30 fractions using a linear accelerator equipped with an on-board imaging system (Varian Medical Systems). Patients were positioned on the couch according to skin tattoos with a standard heel and knee fixation and CBCT was performed. After registration of the CBCT to the planning CT patients were moved into treatment position. In order to assess the residual rotational set-up error we re-matched the CBCT and CT scans allowing only for pitch, roll and yaw. We used the pitch, yaw, and the distance from the isocenter to the cranial and caudal borders of the CTV to calculate the target displacement in the most cranial and caudal regions.

Results: In 45 of the 650 treatment fractions the residual pitch and yaw errors resulted in a displacement larger than 5 mm in the most cranial region. Four patients alone accounted for 28 of these fractions having between 5 and 10 fractions with displacements >5 mm. For the remaining 21 patients none had more than 3 fractions with displacements >5 mm during the treatment course. In the caudal region of the treatment field only 25 fractions with displacements > 5 mm were observed. In this case a single patient accounted for 11 of these treatment fractions. Ten of the studied patients had no target displacements larger than 5 mm in either of the investigated directions.

Conclusion: Our study shows that the use of daily CBCT scans to position patients in the translational directions is effective in terms of reducing set-up errors. In most patients the residual rotational errors will not result in under-dosage of the target in cranial and caudal regions when using a 5 mm PTV margin. However, in a few patients there is a more systematic rotational component giving rise to displacements larger than 5 mm in a significant number of fractions.

Identifying hypoxia in human tumors: a correlation study between FMISO PET and the Eppendorf oxygen electrode

S. Buus[a], L.S. Mortensen[a], M. Nordsmark[a] ,L. Bentzen[a], O.L. Munk[b], S. Keiding[b], J. Overgaard[a] *[a]Department of Experimental Clinical Oncology, Aarhus University Hospital (AUH), Aarhus, Denmark. [b]PET Centre, AUH, Denmark.*

Introduction: Numerous attempts have been made to identify tumor hypoxia. Polarographic oxygen electrodes have been widely used and have demonstrated prognostic significance of hypoxia. However, its routine application is limited. FMISO PET scans are a noninvasive approach, able to measure spatial and temporal changes in hypoxia. The aim of this study was to examine the association between volumes of hypoxia defined by functional imaging and Eppendorf Electrodes.

Materials and methods: A total of 18 patients were included in this study, 9 patients with squamous cell carcinoma (6 with head and neck cancer/3 with unknown primary tumor) and 9 with soft tissue tumors (5 sarcomas/4 benign tumors). The tumor volume was defined by CT or MR. The oxygenation status of the tumors was assessed using FMISO PET imaging followed by Eppendorf Electrode measurements. For FMISO PET 218-462 (median 394) MBq was administered, and images were acquired ~212 minutes (range 150-249 min.) after injection. With the Eppendorf Electrode an average of 109 (range 56 – 230) measurements from 6 (range 4-10) tracks were made per tumor.

Results: Tumors had a median pO_2 value of 6.6 mmHg (range 0.7 – 20 mmHg). The median percentages of pO_2 values below or equal to 2.5 mmHg and 5 mmHg were 26% (range 0 to 62%) and 43 % (range 9 – 93%) respectively. For FMISO PET the median standardized uptake value (SUV_{med}) was 1.4 (range 1.0-2.1), the SUV_{min} was 0.6 (range 0.1-1.4) and the SUV_{max} was 2.6 (range 1.4-6.0). From these results, tumors could be categorized in 3 groups: tumors with high FMISO uptake and low pO_2, tumors with low FMISO uptake and high pO_2, and tumors with low FMISO uptake and low pO_2,

Conclusion: Based on this study**,** there was sometimes a lack of association between hypoxia defined by FMISO PET and Eppendorf Electrodes. This could result from the limited number of cases and a heterogeneous case mix of patients, but may also reflect some measurements being made from necrotic areas of the tumors.

Non-invasive imaging of combretastatin activity in different tumour models: association with more invasive estimates

Thomas Nielsen[1,2] , Rumi Murata[1] , Ross J. Maxwell[3] , Hans Stødkilde-Jørgensen[4] , Leif Østergaard[2], Carsten D. Ley[5] , Paul E. G. Kristjansen[5] , Michael R. Horsman[1]. *[1]Dept. Experimental Clinical Oncology and [2]Dept. Neuroradiology, Center of Functionally Integrative Neuroscience, Aarhus University Hospital, Aarhus, Denmark; [3]University of Newcastle Upon Tyne, Northern Institute for Cancer Research, Newcastle upon Tyne, UK; [4]MR Research Centre, Aarhus University Hospital, Aarhus, Denmark [5]Dept. Biomedical Sciences, University of Copenhagen, Copenhagen, Denmark.*

Introduction: Different studies have shown that the efficacy of the vascular disrupting agent combretastatin A-4 disodium phosphate (CA4P) can depend on a range of different factors including tumour size, nitric oxide, interstitial fluid pressure, and vascular permeability. These factors vary among tumour types. The aim of this study was to investigate all these factors in two tumour models previously shown to respond differently to CA4P with focus on the information obtainable by in vivo imaging.

Materials and Methods: C3H mammary carcinomas and KHT sarcomas were grown to volumes of 200 to 800 mm^3 and treated with CA4P intraperitoneally at a dose of 100 mg/kg. Tumour size and the effect of a nitric oxide inhibitor nitro-L-arginine (NLA) administered intravenously were evaluated by necrotic fraction assessed by histology. Interstitial fluid pressure (IFP) was measured using the wick-in-needle technique, and vascular characteristics were assessed with dynamic contrast enhanced magnetic resonance imaging (DCE-MRI).

Results: Initial necrotic fraction was about 10% in both tumours at 200 mm^3, but only increased with tumour size in the C3H mammary carcinoma. In the C3H tumour, CA4P induced further necrosis (about 15% of tumour volume) at all sizes, but in the KHT tumour, the induced necrotic fraction depended on tumour size. The increase in necrotic fraction caused by NLA given together with CA4P was higher than the sum of the induced necrotic fractions induced by each drug given alone. CA4P significantly decreased IFP in all tumours except in the 800 mm^3 C3H tumour, which had an initially lower value (although not significantly). Interstitial volume estimated by DCE-MRI indicated an increase in all groups except the in the 800 mm^3 C3H tumour. IFP decrease and interstitial volume increase seemed related. DCE-MRI vascular parameters showed different initial characteristics and general significant reductions following CA4P treatment.

Conclusions: The two tumour models showed differences in all investigated factors before treatment as well as in their response to CA4P. Perfusion and permeability as estimated by DCE-MRI plays a central role in the CA4P response, and IFP decrease and DCE-MRI interstitial volume increase seemed related. The investigated factors may be of clinical value in the planning of CA4P treatments.

Supported by grants from Danish Cancer Society and the Danish Research Agency

Influence of the fixation and imaging protocol on the treatment margin for thoracic patients – a multi centre study.

Nielsen, T.B.[1,2], Westberg, J.[1], Hansen, V.N.[3], Brink, C.[1,2] *[1]Laboratory of Radiation Physics, Odense University Hospital, DK-5000 Odense, Denmark. [2]Faculty of Health Sciences, University of Southern Denmark, Odense, Denmark. [3]Royal Marsden Hospital, Sutton, Surrey SM1 5PT, United Kingdom.*

Purpose/Objectives: Knowledge of the tumour position over the entire treatment course is crucial in order to apply small margins to be used with highly modulated treatment techniques. A previous study based on Cone-Beam CT (CBCT) of 77 patients (Bertelsen et al, Acta Oncol 2009-48:259) showed that the overall patient position uncertainty increases during the treatment course which can be addressed by adapted treatment planning. The aim of this study is to identify and compare systematic and random errors for different immobilization techniques and imaging protocols using the exact same analysis techniques and investigate whether any differences could impact on the applied margins.

Materials/methods: Measurements of translational and rotational shifts based on CBCT scans were collected and evaluated retrospectively from The Royal Marsden Hospital (RMH) and Odense University Hospital (OUH) with a total of 327 thorax patients (2270 CBCT scans). Patients treated at RMH were immobilised using either a wing board or a breast board, some of the breast board patients were treated with Active Breathhold Control. Patients at OUH were fixated using customized vacuum cushions (VacFix) and a full thermoplastic mask (AquaPlast) from the chin to the umbilicus. CBCT scans were performed at the three first fractions and several times during the treatment course using Elekta Synergy accelerators.

Results: An overall good patient positioning accuracy is found for both fixation systems in the rotational directions with random errors at 1.10-1.20 degrees at RMH and 0.55-0.89 degrees at OUH. Larger systematic translational errors are observed at both centres in the CC direction compared to AP and LR. Differences between RMH and OUH are observed for the translational errors with 0.37cm in LR and CC direction at RMH and 0.20cm and 0.31cm at OUH. On-going analyses investigate the potential drift of fixation equipment during a treatment course for each centre. The results may influence future treatment margins for thorax tumours.

Conclusion: The small rotational values validate the clinical procedures using a table correction only in the translational direction. The larger errors in the CC direction indicate a general problem in fixating thorax patients in the CC direction. Further analyses and statistical tests will be performed to reveal any other differences between the different fixation systems.

IGRT in squamous cell carcinoma esophageal cancer – experiences with cone beam CT

M Nordsmark[1], A Vestergaard[2], M Knap[1], L Hoffmann[2]. *[1]Aarhus University Hospital, Department of Oncology, Aarhus, Denmark. [2]Aarhus University Hospital, Department of Medical Physics, Aarhus, Denmark.*

Introduction: The purpose of this study was to explore the possibilities of IGRT with cone beam CT (CBCT) in esophageal cancer. The differences between setup strategies using external landmarks, bony anatomy match or tumor match was investigated as well as tumor shrinkage during radiotherapy.

Materials and Methods: Eight consecutive patients treated with curative neoadjuvant chemotherapy (CH) & concomitant chemoradiotherapy (CH-RT) had daily cone beam CT and were treated according to bony anatomy match. Four patients received preoperative induction cisplatin-5FU followed by weekly cisplatin & continuous 5-FU during RT 45Gy/25 fx. Four patients received definitive CH-RT, 50-60Gy/25-30 fx, cisplatin day 1, 22 & 43 and continuous 5-FU during RT. All patients had intensity modulated RT (IMRT). The median time from planning CT until RT start was 17.5 days (range 8-21), & the median time from first CH to planning CT was 5.5 days (range 2-13). A total of 206 cone beam CT scans were matched off-line on tumor site, GTV-T as delineated on the planning CT. GTV-T was delineated on CBCT day 1(GTV-1F) mid treatment and last day of treatment. GTV-T was measured on plan CT and the 3 CBCT's and the GTV-1F/GTV-T ratios were calculated.

Results: The max systematic deviation obtained aligning patients after skin marks and bony anatomy match was 6 mm in all three directions, n=8 pts. Random setup errors were up to 10 mm. Comparing match on bony anatomy and soft tissue in 2 cases using the GTV-T volume the difference was > 5 mm in all directions during the entire course of treatment, the median being > 1 mm. Five patients had deviations up to 7 mm and in 1 case the deviation was of up to 10 mm. Two patients among 4 having preoperative CH followed by CH-RT presented a reduction of the GTV at CBCT day 1 compared to GTV plan CT (GTV-1F/GTV-T ratio of 0.72 and 0.87 respectively), while two patients showed no change. GTV-1F/GTV-T ratios of 4 patients receiving definitive chemo/XRT were 0.83, 0.88, 0.96 and 0.97. Further during treatment data will be presented.

Conclusion: Aligning patients after bony anatomy was in favor of using skin marks. There was a systematic difference between matching on bony anatomy and soft tissue. Induction CH may induce tumor shrinkage and impact on GTV-T if the time interval between CH & plan CT is too short. These findings may advocate for the use of adaptive RT in esophageal cancer.

Single institution experience from 100 patients included in Danish Breast Cancer Cooperative Group (DBCG) radiation protocols: compromise is necessary between dose to the left anterior descending coronary artery and breast clinical target volume

[1]Offersen BV, [1]Overgaard M, [2]Thomsen MS, [1]Grau C, [3]Overgaard J. *[1]Dept. Oncology, [2]Dept. Medical Physics, [3]Dept. Experimental Clinical Oncology, Aarhus University Hospital, Aarhus, Denmark.*

Introduction: Radiation-induced heart disease may offset the improvements in disease-specific survival provided by adjuvant breast radiotherapy (RT). Thus, for adjuvant breast RT minimizing dose to the heart is critical. No consensus indicates which region in the heart is most important for radiation-induced morbidity. In DBCG guidelines heart V20 (normofractionated RT) and V17 (hypofractionated RT) is 10% and V40 (normofractionated) and V35 (hypofractionated RT) is 5% Gy, and since May 2009 max 17 Gy to the left anterior descending coronary artery (LADCA) has been recommended.

Materials and Methods: The first 100 patients included in DBCG HYPO protocol (randomization 50 Gy / 25 fr (38pts) versus 40 Gy / 15 fr (34pts)) and PBI protocol (partial breast irradiation, 40 Gy / 15 fr, randomization whole breast (17pts) versus partial breast (11pts)) at our institution are evaluated. All patients were treated with adjuvant RT to residual breast only. Breast CTV, heart V17, V20, V35 and V40, max dose to LADCA and percentage CTV breast treated to a dose <95% are reported. Updated data will be provided at the meeting.

Results: Left versus right sided breasts were treated in 59 versus 41 patients. Median CTV breast was 598 ml (range, 97-1956 ml). For left versus right sided RT plans median LADCA dose was 17.2 Gy (range, 0.39-51.3 Gy) vs. 0.24 Gy (range, 0-1.7 Gy). From May to Nov 2009, 47pts were treated, and 53pts were treated from Nov 2009 to Febr 2010. For left sided RT plans in the first period, mean LADCA dose was 24.2 Gy (SD 16.1 Gy) and in the late period 18.7 Gy (SD 9.1 Gy), p=0.10 (t-test). Mean CTV breast with dose <95% in the first period was 2.92% (SD 2.99%) and in the last period 5.52% (SD 3.24%), P=0.003 (t-test). In all cases heart V17, V20, V35 and V40 were below 10 and 5%, respectively. In the first period LADCA constraints were violated in 16 cases vs. 14 cases in the last period.

Conclusions: In order to shield dose to LADCA the anterior part of the heart has been eliminated from the RT fields causing a significant increase in the volume of breast CTV treated to a dose <95%. As the prognosis after therapy for early breast cancer is increasing it is even more important to strive towards as few side effects as possible. However, this may jeopardise target volume coverage. Solutions to this problem include image-guided radiotherapy and organ motion management.

On the potential use of alanine for small field output factor determination in high energy photon beams - A Monte Carlo study.

R O Ottosson[1,2], C F Behrens[1], J Helt-Hansen[2], C E Andersen[2]. *[1]Copenhagen University Hospital Herlev, Department of Oncology (R), Division of Radiophysics (52AA), Herlev. Ringvej 75, DK--2730 Herlev, Denmark. [2]Risø-DTU, Risø High Dose Reference Laboratory, Technical University of Denmark, Roskilde, Denmark.*

Introduction: For small field dosimetry, three main issues are of concern: lack of lateral charged particle equilibrium (CPE), volume averaging and fluence perturbation introduced by the detector. With the introduction of radiosurgery and dynamic treatments, the delivered beams, or beam segments, have become smaller. Thus, there is an increased need to correctly measure output factors (OF) for small fields. Alanine is a suitable choice of detector material since it exhibits physical properties in close agreement with water and a linear dose response. Furthermore it is possible to produce small alanine detectors. This study investigates the potential use of alanine pellets, of various sizes, for determination of OFs for small high energy photon fields (0.6x0.6 – 5x5 cm^2).

Material and Methods: An MC model of a 6 MV Varian 2300 iX was built and commissioned using EGSnrc/BEAMnrc. MC simulations of a Gammex solid water phantom were conducted with and without a voxel representing the alanine dosimeter present. The dosimeter volume was varied between 2.5x2.5x2.5 and 10.0x10.0x2.5 mm^3. OFs at 10 cm depth (SSD = 90 cm) and the cavity theory factor, *f(Q)*, were calculated.

Results: For field sizes larger than 3x3 cm^2, OFs for all detector sizes were in agreement with the homogeneous phantom. For smaller field sizes the detector volume starts becoming important. Even the smallest detector volume showed a small under response, due to the perturbation, but was able to reproduce the OFs within an uncertainty of 0.5% for field sizes larger than 1x1 cm^2 (table 1). Moreover *f(Q)* was constant, within 0.6%, over the full range of studied field sizes.

Conclusions: Alanine detectors, with a volume of 2.5x2.5x2.5 mm^3, are suitable for OF determination of small fields is solid water, as suggested by the constant *f(Q)*. Considering the linear dose response, alanine is potentially useful in small field dosimetry. Reducing the pellet volume will decrease the perturbation, but increase the inaccuracy as the read out signal intensity will be decreased. Prior to adopting an alanine based dosimetry protocol, measurements in actual water will need to be conducted.

Supported by CIRRO - The Lundbeck Foundation Center for Interventional Research in Radiation Oncology and The Danish Council for Strategic Research.

Evaluation of NSCLC patient setup accuracy by investigating 3 and 6 degrees-of-freedom CBCT auto matches, based on whole thorax, columna vertebralis and GTV

Ottosson W[1], Baker M[1], Hedman M[2,3], Sjöström D[1]. *[1]Department of Oncology (R), Division of Radiophysics (51AA), Copenhagen University hospital, Herlev, Denmark. [2]Department of Oncology (R), Copenhagen University hospital, Herlev, Denmark. [3]Department of Oncology-Pathology, Karolinska Institutet, Stockholm, Sweden.*

Introduction: Image guided radiotherapy (IGRT) are used in modern radiotherapy to ensure encompassing the target by prescribed dose while sparing normal tissue. Orthogonal 2D kV images are well suited for bone match, in contrast to soft tissue. Utilizing a 3D cone-beam CT (CBCT) instead for patient setup verifications enables performing matches on different types of structures, and assessing the consequences of rotational shifts.
The aim was to evaluate the patient setup accuracy by different types of CBCT matches, and to investigate the influence on the translational shifts when using 3 or 6 (including rotations) degrees-of-freedom (DOF).

Materials and methods: Totally 15 NSCLC patients were enrolled in this study. Initial setup was performed by aligning the patient's skin tattoos to the room lasers, and later weekly CBCT scans were acquired. An evaluation of the positional errors, when using the patient's skin tattoos without image guidance for patient setup, compared to acquired CBCT auto match on; the whole thorax, the columna vertebralis, or the GTV, were performed. Consequently, the resulting couch shifts and patient rotations in three dimensions were assessed. The parameters of the GTV match were used as the golden standard. Furthermore, the setup accuracy of using 3 or 6 DOF was investigated.

Results: A 3 DOF auto match of the whole thorax, compared to the GTV match, resulted in systematic (Σ) and random (σ) translational errors of 0.6-1.5 mm and 0.8-1.4 mm, respectively. On the other hand the columna vertebralis 3 DOF match, resulted in Σ of 0.9-1.9 mm and σ of 0.8-1.2 mm. Eventually, no image guidance setup resulted in Σ of up to 2.0-3.3 mm and σ of 1.8-3.2 mm. When comparing the 3 and 6 DOF matches, a significant ($p < 0.05$) difference in the longitudinal direction was retrieved for the whole thorax, but only a minor difference for the related 3D-vector was obtained. There were also significant differences in the vertical and lateral directions for the columna vertebralis match and the no image guidance setup. But for the related 3D-vectors, only the columna vertebralis match yields considerable difference.

Conclusion: Image guidance for NSCLC is essential, since only tattoo setup yields significant difference from GTV match. On the other hand, the whole thorax and columna matches results in approximately the same translational errors.

Influence of MLC leaf width on biologically adapted IMRT plans

Rødal J [1,2], Søvik Å [1,3], Malinen E [1]. *[1]Dept. of Medical physics, Norwegian Radium Hospital, Oslo University Hospital. [2]Dept. of Physics, Norwegian University of Science and Technology, Trondheim. [3]Dept. of Companion Animal Clinical Sciences, Norwegian School of Veterinary Science, Oslo.*

Introduction: High resolution medical images for biology-guided adaptive therapy may require high resolution beam delivery for optimal treatment. In this work, we have studied the influence of multi leaf collimator (MLC) leaf width on the treatment outcome following adapted IMRT of a hypoxic tumor.

Material and methods: Dynamic contrast enhanced MR images of a dog with a spontaneous tumor in the nasal region were used to create a tentative hypoxia map following a previously published procedure. The hypoxia map was used as a basis for generating compartmental gross tumor volumes (GTVs), which were utilized as planning structures in biologically adapted IMRT. The KonRad inverse treatment planning system (Siemens Medical Solutions) was used for dose planning. Three different MLCs were employed, with leaf widths of 2.5, 5 and 10 mm. The number of treatment beams and the degree of step-and-shoot beam modulation were varied. By optimizing the tumor control probability (TCP) function, optimal compartmental doses were derived and used as target doses in the inverse planning. Resulting IMRT dose distributions were exported and analyzed, giving estimates of TCP and compartmental equivalent uniform doses (EUDs). The impact of patient setup accuracy was also simulated.

Results: The MLC with the smallest leaf width (2.5 mm) consistently gave the highest TCPs and compartmental EUDs, assuming no setup error. The difference between this MLC and the one with 5 mm width was rather small though, while the MLC with 10 mm width gave considerably lower TCPs. When including random setup errors, the same trend was found. However, for systematic setup errors larger than 3 mm, only minor differences were seen between the MLCs.

Conclusions: Biologically adapted radiotherapy may require MLCs with leaf widths smaller than 10 mm. However, for a high probability of cure it is crucial that accurate patient setup is ensured.

Comparison of manual and automatic segmentation for FDG-PET based tumor delineation in head and neck cancer

Sand H1, Prakash V2, Carl J1. *1) Department of Medical Physics, Oncology, Aalborg Hospital, Denmark. 2) Department of Nuclear Medicine, Aalborg Hospital, Denmark.*

Introduction: Intensity-modulated radiotherapy in the context of image-guided radiotherapy in head and neck cancer (HNC) requires accurate definition of target volumes. Functional imaging using 18F-fluorodeoxy-glucose (FDG) positron emission tomography (PET) has demonstrated a high degree of accuracy in gross target volume (GTV) delineation. Unfortunately, since PET images are hampered by relatively poor spatial resolution, large quantities of statistical noise, and non-specific patterns of FDG uptake, manual target delineation is still the most used in clinical routine. However, this method can be very inconsistent and may have poor reproducibility. Many factors account for this. Some are operator variability, diverse patterns of uptake within and between patients compounded by tumor heterogeneity and non standardization of display window viewing conditions. Of the studies in HNC published to date, automated GTV segmentation has typically been threshold-based, either as a fixed threshold of the maximum standard uptake value within the perceived tumor volume or as an adaptive threshold of the signal-to-background ratio. Differences in the identified GTV which result between these methods can be substantial and clinically significant. However, the appropriate use of advanced image-processing tools like denoising and deblurring techniques can address the noise and esolution issues of the PET images, allowing the use of more advanced segmentation methods. At Université St. Luc in Brussels, Belgium, a gradient-based method has been developed relying on the watershed transform and cluster analysis for segmenting denoised and deblurred FDG PET images [1]. The method has shown good results compared to delineations performed on pathological specimens of laryngeal tumors. Our study compares manual delineation and a threshold segmentation technique with the gradient-based method on histologically confirmed HNC.

Materials and methods: Taking the gradient-based method [1] as a benchmark, a comparison of delineations performed on 20 HNC patients based on visual interpretation, a threshold-based technique and the gradient-based method will be given. The absolute GTVs, the overlap between GTVs and a measure of the maximum and minimum distance between the GTVs will be shown. A detailed description of the three different segmentation methods including advantages and disadvantages will also be presented.

[1] Geets X, Lee JA, Bol A, Lonneux M, Grégoire V. *A gradient-based method for segmenting FDG-PET images: Methodology and validation.* Eur J Nucl Med Mol Imaging 2007;34:1427-1438

Dose calculation in biological samples in a mixed neutron-gamma-field at the University of Mainz

T. Schmitz[1], M. Blaickner[2], C. Schütz[1], N. Wiehl[1], J.V. Kratz[1], N. Bassler[3], M. Holzscheiter[4], G. Hampel[1]. *[1]Institute for Nuclear Chemistry, University of Mainz, D-55099 Mainz, Germany. [2]AIT Austrian Institute of Technology GmbH, 2444 Seibersdorf, Austria. [3]Department of Experimental Clinical Oncology, Aarhus University Hospital, Aarhus, Denmark. [4]Department of Physics & Astronomy, University of New Mexico, Albuquerque, NM 87131-0001, USA.*

Introduction: To establish Boron Neutron Capture Therapy (BNCT) for non-resectable liver metastases and for in vitro experiments at the TRIGA Mark II reactor at the University of Mainz, Germany, it is necessary to have a reliable dose monitoring system. The in vitro experiments are used to determine the relative biological effectiveness (RBE) of liver and cancer cells in our mixed neutron and gamma field, which is crucial for the planned liver treatment.
We work with alanine detectors in combination with Monte Carlo (MC) simulations, where we can measure and characterize the dose attributed to the direct photon component and the long range secondary charged particles from neutron reactions. To verify our MC-calculations we perform neutron flux measurements using gold-foil activation and pin-diodes. The neutron flux together with the alanine detectors and the Monte Carlo calculations eventually lead to a reliable and accurate dosimetry planning protocol.

Materials and Methods: The alanine pellets have a diameter of 5 mm and a thickness of 2 mm, consisting of 90% finely grained crystalline alanine powder. L-α-alanine is an amino acid which occurs naturally in the human body. When alanine is irradiated with ionizing radiation, it forms the stable radical CH_3–C·H–COOH which can be detected by using an electron spin resonance (ESR) reader. The value of the ESR signal correlates to the amount of absorbed dose. The irradiations take place at the TRIGA Mainz. The reactor can be operated in the steady state mode with a maximum power of 100 kW_{th}. It has a thermal column which can be reconstructed for the treatment of an explanted organ and is used for the dosimetric and in vitro measurements.
The dose for each pellet is calculated using FLUKA, a multipurpose Monte Carlo transport code, able to treat particle interactions up to 10000 TeV. The pin-diode consists of lithium fluoride foil. This foil converts the neutrons into alpha and tritium particles which are products of the $^{7}Li(n,\alpha)^{3}H$-reaction. These particles are detected by the diode and their amount correlates to the neutron fluence directly.

Results and Discussions: We find the gold foil activation and the pin diode are reliable fluence measurement systems for our reactor. Alanine dosimetry of the photon field and charged particle field from secondary reactions can in principle be carried out in conjuction with MC-calculations for mixed radiation fields and the Hansen&Olsen alanine detector response model. With the acquired data about the background dose and charged particle spectrum, and with the acquired information of the neutron flux, we are capable of calculating the dose to tumour as a function of the local boron concentration. Currently we also speculate on sensitizing alanine by adding boron compounds, which further can be used in future experiments to improve dosimetry methods. Monte Carlo simulation of the mixed neutron and gamma field of the TRIGA Mainz is possible in order to characterize the neutron behavior in the thermal column.

A phantom treatment planning study of the distribution of dose-averaged LET in small volumes irradiated with ^{12}C.

Søndergaard C. S. , Petersen,J. B. B., Jäkel, O. and Bassler, N. *Department of Medical Physics, Aarhus Sygehus, Aarhus University Hospital, DK-8000 Aarhus C, Denmark. Deutsches Krebsforschungszentrum (DKFZ), Medizinische Physik, DE-69120 Heidelberg, Germany. Department of Physics and Astronomy, Aarhus University, DK-8000 Aarhus C, Denmark.*

Introduction: Irradiation with carbon ions is a promising approach to hypoxia-based selective boosting or dose painting, due to the high relative biological effect (RBE), and low oxygen enhancement ratio, at the end of the ions ranges. In the extreme limit of dose painting, the segmentation of the target volume based on some biologically sensitive imaging technique could result in a large number of disjunct subvolumes with complex geometrical shapes, large variation in size and spacing to neighbouring subvolumes. As a consequence of the strong variation of the linear energy transfer (LET) of heavy ion irradiation in the vicinity of the Bragg peak, the dose-averaged LET (LET_D) distribution in small volumes will be sensitive to variation in size, shape and position. Here, we study this effect in a simple simulated geometry with ^{12}C fields and uniform physical dose optimization. The results illustrate how LET_D is diluted when the size of the target volume is increased, and how multiple fields improve the uniformity of the LET_D distribution.

Materials and Methods: The planning study is performed with the TRiP98 code on a simulated (20x20x20 cm^3) water equivalent phantom with a target of variable volume (8 – 64000 mm^3) at the centre. Beams of ^{12}C with parameters from the therapy beamline at the SIS accelerator at GSI is optimized to uniform physical dose. The LET_D distribution within the target is calculated and evaluated.

Results: The LET_D is less the larger the volume; the mean value is reduced from 160 keV/µm at 2x2x2 mm^3 to 60 keV/µm at 40x40x40 mm^3. A four field geometry compared to a single field improves the uniformity; with a single field the span is 60-190 keV/µm at 10x10x10 mm^3, which reduces to 90-120 keV/µm with four fields.

Conclusions: The high LET_D values, > 150 keV/µm, at the smallest volumes, < 5x5x5 mm^3, is in a biologically interesting range where the RBE peaks and the OER falls to unity. For larger volumes the effect is diluted. A uniform LET_D distribution, allowing a robust mapping from physical dose to biological effect, can be approached using multiple field directions.

A study of image-guided radiotherapy of bladder cancer based on Lipiodol injection in the bladder wall.

Søndergaard J1, Olsen KØ2, Muren LP1,3, Elstrøm UV1,3, Grau C1 and Høyer M1. *1Department of Oncology, Aarhus University Hospital, Aarhus, Denmark. 2Department of Urology, Aarhus University Hospital, Aarhus, Denmark. 3Department of Medical Physics, Aarhus University Hospital, Aarhus, Denmark.*

Purpose: We have tested a procedure of focal injection of the contrast medium Lipiodol as a fiducial marker for image-guided boost of the tumor in bladder cancer radiotherapy (RT). In this study, we have evaluated the feasibility and the safety of the method as well as the inter- and intra-fraction shift of the bladder tumor.

Materials and methods: Five patients with muscle invasive urinary bladder cancer were included in the study. Lipiodol was injected during flexible cystoscopy into the submucosa of the bladder wall at the periphery of the tumor or the post resection tumor-bed. Cone-beam CT (CBCT) scans were acquired daily throughout the course of RT.

Results: Lipiodol demarcation of the bladder tumor was feasible and safe with only a minimum of side-effects related to the procedure. The Lipiodol spots were visible on CT and CBCT scans for the duration of the RT course. More than half of all the treatment fractions required a geometric shift of 5 mm or more to match on the Lipiodol spots. The mean intra-fraction shift (3D) of the tumor was 3 mm, largest in the anterior-posterior and cranial-caudal directions.

Conclusion: This study demonstrates that Lipiodol can be injected into the bladder mucosa and subsequently visualised on CT and CBCT as a fiducial marker. The relatively large inter-fraction shifts in the positions of Lipiodol spots compared to the intra-fraction movement indicates that image-guided RT based on radio-opaque markers is important for RT of the bladder cancer tumor.

IDENTIFYING pH INDEPENDENT HYPOXIA INDUCED GENES IN HUMAN SQUAMOUS CELL CARCINOMAS IN VITRO

Brita Singers Sørensen, Kasper Toustrup, Michael R. Horsman, Jens Overgaard, Jan Alsner
Department of Experimental Clinical Oncology, Aarhus University Hospital, Aarhus, Denmark.

Background: Genes upregulated by low oxygen have been suggested as endogenous markers for tumor hypoxia. Yet, most of the genes investigated have shown inconsistent results, which have led to concerns about their ability to be true hypoxia makers. Previous studies have demonstrated that expression of hypoxia induced genes can be affected by extracellular pH (pH_e).

Methods: Five different human cell lines (SiHa, $FaDu_{DD,}$ UTSCC5, UTSCC14 and UTSCC15) were exposed to different oxygen concentrations and pH (7.5 or 6.3), and gene expression analyzed with microarray (Affymetrix - Human Genome U133 Plus 2.0 Array).

Results: An analysis of two of the cell lines using SAM identified 461 probesets that were able to separate the four groups “Normal oxygen, normal pH” “Low oxygen, normal pH” “Normal oxygen, low pH” “Low oxygen, low pH”. From here it was possible to identify a fraction of probesets induced at low oxygen independent of pH in these two cell lines, this fraction included HIG2, NDRG1, PAI1 and RORA. Further verification by qPCR highlighted the necessity of using more cell lines to obtain a robust gene expression profiles.
To specifically select pH independent hypoxia regulated genes across more cell lines, data for $FaDu_{DD,}$ UTSCC5, UTSCC14 and UTSCC15 were analyzed to identify genes that were induced by hypoxia in each cell line, where the induction was not affected by low pH, and where the gene was not significantly induced by low pH alone. Each cell line had 65-122 probesets meeting these criteria. For genes to be considered as target genes (hypoxia inducible pH independent), genes had to be present in three out of four cell lines.

Conclusion: The result is a robust hypoxia profile unaffected by pH across cell lines consisting of 27 genes. This study demonstrates a way to identify hypoxia markers by microarray, where other factors in the tumor microenvironment are taken into account.

Propagation of target and organ at risk contours in prostate radiotherapy using deformable image registration

Sara Thörnqvist[1,2], Jørgen BB Petersen[3], Lise N. Bentzen[4], Morten Høyer[4] and Ludvig Paul Muren[1,2]. *[1]Departments of Oncology and Medical Physics, Aarhus University Hospital, Aarhus, Denmark.[2]Clinical Institute, Aarhus University, Aarhus, Denmark. [3]Department of Medical Physics, Aarhus University Hospital, Aarhus, Denmark . [4]Department of Oncology, Aarhus University Hospital, Aarhus, Denmark.*

Introduction: Successful deformable image registration is an important tool in the development of advanced radiotherapy (RT), with its main applications being in adaptive RT, enabling treatment adaptation and dose accumulation despite large anatomical changes. The aim of this study was to evaluate the performance of a deformable image registration application for propagation of target and organ at risk contours in prostate RT, a region where considerable deformations are expected.

Material and Methods: The study involved four prostate cancer patients previously treated with IMRT who had 9-11 repeat CT-scans evenly distributed throughout their treatment. A radiation oncologist contoured the prostate, pelvic lymph nodes, rectum and bladder in all CT-scans. The repeat CT-scans were retrospectively registered to the initial CT using both rigid and deformable registration. All registrations were performed in a non-released commercial clinical software system. The rigid registrations were based on bony anatomy (200-3000 HU), only considering translations and with a volume of interest (VOI) covering the entire CT-scan. Two deformable registration algorithms were used (A and B), the latter incorporating pre-known knowledge of the deformations. Following the rigid registrations, all deformable registrations were made with a ROI enclosing the Sup-Inf extension of the rectum. The results were evaluated based upon the Dice similarity coefficient (DSC).

Results: Deformable registration improved the DSC for the considered organs in 87% and 81% of the registrations with algorithm A and B, respectively. The largest increase in mean DSC relative the rigid registrations was seen with the algorithm A for bladder and rectum, both with a mean increase of 13%, compared to a 2% increase with the algorithm B. These values correspond to a mean DSC for all patients of 0.78 and 0.89 for rectum and bladder with algorithm A and 0.71 and 0.81 for rectum and bladder with algorithm B. For the prostate a mean relative increase in DSC was 6% and 4% corresponding to a mean DSC for all patients of 0.85 and 0.84 with algorithm A and B, respectively. The smallest change in DSC was seen for the pelvic lymph nodes, with a mean relative increase of 1% with both algorithms, although this target was only partly covered in the deformation.

Conclusions: Deformable registration was found to improve the DSC for all organs considered, with the highest increase in mean DSC for rectum and bladder. The results further indicate algorithm B to be more restricted to the input from the rigid registration.

The project was supported by Varian Medical Systems, Palo Alto, CA, USA.

Stereotactic body radiotherapy: Relationship of setup errors to body mass index and treatment time

Worm E.S., Hansen A.T., Petersen J.B.B., Præstegaard L.H., and Høyer M. *Department of Oncology, Aarhus University Hospital, Aarhus, Denmark.*

Introduction: The purpose of this study is to evaluate setup errors for stereotactic body radiotherapy (SBRT) in a Varian clinic in a 3D plan-CT setting. Correlations between setup errors and sex, age, body mass index (BMI), and treatment time are investigated to determine whether they influence on the benefit of daily image guidance.

Materials and methods: From October 2008, a CBCT was acquired before and after each of three treatment fractions for patients receiving SBRT for tumors in the lung and liver. All patients (18 lung, 18 sites and 15 liver, 16 sites) were immobilized and positioned using a stereotactic body frame (Elekta). CBCT scans were registered with bony anatomy of the planning CT, to find patient positioning errors (PPE). For lung patients, registration was also performed on tumor, to find the baseline shift compared to bony anatomy. All image registrations were performed in Varian Offline Review using the features of automatch on bony anatomy and soft tissue automatch on "GTV+1cm" (only lung tumors). Correlation analysis was perfomed using Spearman's non-parametric regression.

Results: For lung and liver sites (n = 34) the interfraction systematic PPE's (1 SD) were 2.1 (LR), 3.7 (CC) and 1.5 mm (AP). Random errors were 1.9, 2.3 and 1.4 mm. Intrafraction PPE's were 0.8, 0.6 and 0.7 mm (systematic) and 0.8, 0.9 and 0.7 mm (random). Interfraction baseline shifts for the lung patients were 1.1, 2.9 and 2.9 mm (systematic) and 0.8, 1.7, and 1.6 mm (random). Intrafraction baseline shifts were 0.9, 0.5 and 0.7 mm (systematic) and 0.7, 0.7 and 0.7 mm (random). A significant correlation ($r_s = 0.44$, $p = 0.014$) between the mean 3D interfraction PPE and BMI was found (n = 31, for three patients BMI was unknown). No correlation ($p = 0.43$) was found between intrafraction PPE and BMI. Total treatment time and intrafraction PPE showed weak, but significant, correlation ($r_s = 0.35$, $p < 0.001$). No correlations were found between PPE and age, sex or between intrafraction baseline shifts and treatment time.

Conclusions: Daily IGRT reduces setup errors considerably, especially for patients with large BMI. Intrafractional errors are small and independent of BMI. Correlation between overall treatment time and intrafraction PPE shows that the treatment time should be kept as short as possible. For the lung patients, baselineshifts demonstrate the necessity for online soft tissue matching.

Acknowledgement: Supported by CIRRO - The Lundbeck Foundation Center for Interventional Research in Radiation Oncology and The Danish Council for Strategic Research.

List of participants (per May 19, 2010)

Thomas Aleksandersen
Student
Department of Medical Physics
Oslo University Hospital
Oslo, Norway
thomasbaleksandersen@hotmail.com

Jan Alsner
Associate professor, PhD
Department of Experimental Clinical Oncology
Aarhus University Hospital
Århus C, Denmark
jan@oncology.dk

Margit Holst Andersen
Nurse
Stråleterapien, Onk. Afd.
Aarhus sygehus
Aarhus C, Denmark
margande@rm.dk

Erlend Andersen
PhD student
Medical physics
Oslo university hospital, Radiumhospitalet
Kristiansand, Norway
andersen.erlend@gmail.com

Nicolaj Andreassen
MD
Dept. of Oncology
Aarhus University Hospital
Aarhus C, Denmark
nicolaj@oncology.dk

Camilla Mondrup Andreassen
Ph.D.-student
Department of Mathematical Sciences
Faculty of science , Aarhus University
Århus C, Denmark
mondrup@imf.au.dk

Marianne Aznar
medical physicist
radiation oncology
Rigshopitalet
Copenhagen, Denmark
marianne.aznar@rh.regionh.dk

Harry Bartelink
prof.dr.
radiotherapy
NKI-AVL
Amsterdam, The Netherlands
h.bartelink@nki.nl

Niels Bassler
post.doc.
Department of Experimental Clinical Oncology
Aarhus University
Aarhus C, Denmark
bassler@phys.au.dk

Claus F Behrens
Research Coordinator
Department of Oncology (R)
Copenhagen University Hospital, Herlev
Herlev, Denmark
clbe@heh.regionh.dk

Lise Bentzen
MD. Ph.D
Dept. of Oncology
Aarhus University Hospital
Aarhus, Denmark
lise@oncology.dk

Mai-Britt Bjørklund Ellegaard
Forskningssygeplejerske
Department of Oncology
Aarhus University Hospital
Århus C, Denmark
maibelle@rm.dk

Carsten Brink
Hospital Physicist
Laboratory of Radiation Physics (afd R)
Odense Universityhospital
Odense, Denmark
carsten.brink@ouh.regionsyddanmark.dk

Robert Bristow
Clinician Scientist
Radiation Oncology
Princess Margaret Hospital - Univ of Toronto
Toronto, Canada
rob.bristow@rmp.uhn.on.ca

Sune Kristian Buhl
Medical Physicist
Department of Oncology
University Hospital of Copenhagen, Herlev
Herlev, Denmark
sukrbu01@heh.regionh.dk

Morten Busk
Ph.D.
Department of Experimental Clinical Oncology
Aarhus University Hospital
Aarhus C, Denmark
morten@oncology.dk

Charlotte Bøje
MD., PHD student
Experimental Clinical Oncology
Aarhus University Hospital
Aarhus C, Danmark
charboej@rm.dk

Annette Bøjen
Leader of the Learning Centre
Department of Oncology
Aarhus University Hospital
Aarhus C, Denmark
annette.boejen@aarhus.rm.dk

Yue Cao
Associate Professor
Radiation Oncology and Radiology
The University of Michigan
Ann Arbor, MI, USA
yuecao@umich.edu

Jesper Carl
Physicist
Dept medical physics
Aalborg Hospital, Århus university Hospital
Aalborg, Denmark
jhc@rn.dk

Christian P. V. Christoffersen
ph.d. student
Computer science
Aarhus University
Aarhus, Denmark
cpvc@cs.au.dk

Stephanie Combs
Dr
Radiation Oncology
Heidelberg University Hospital
Heidelberg, Germany
Stephanie.Combs@med.uni-heidelberg.de

Francisco Cutanda Henriquez
Medical Physicist
Nuclear Medicine
Hospital General Univ Gregorio Marañón
Madrid, Spain
francisco.cutanda@salud.madrid.org

Alexandru Dasu
Medical Physicist
Radiation Physics Department
Linköping University Hospital
Linköping, Sweden
alexandru.dasu@lio.se

Joseph Deasy
Professor and Director
Radiation Oncology
Washington Univ School of Medicine St. Louis
St. Louis, USA
jdeasy@radonc.wustl.edu

Anne Kirkebjerg Due
læge, klinisk assistent (ph.d.-studerende)
Stråleterapiklinikken, afsnit 3994
Rigshospitalet
København Ø, Denmark
anne.k.due@sol.dk

Fréderic Duprez
Radiation Oncologist
Radiotherapy Dept.
Ghent University Hospital
Ghent, Belgium
frederic.duprez@ugent.be

Karsten Eilertsen
Head of Radiotherapy Physics
Dept. of Medical Physics
Oslo Univeristy Hospital - Radiumhospitalet
Oslo, Norway
karsten.eilertsen@radiumhospitalet.no

Ulrik Vindelev Elstrøm
Medical Physicist, PhD-student
Dept. of Oncology & Dept. of Medical Physics
Aarhus University Hospital
Århus C, Denmark
ulrielst@rm.dk

Jesper Grau Eriksen
MD, phd
Dept. of Oncology, R
Odense Universityhospital
Odense C, Denmark
jesper@oncology.dk

Katherina Farr
MD
Clinical Oncology
Aarhus University Hospital
Aarhus, Denmark
katherinanp@hotmail.com

Barbara Malene Fischer
MD
Clinical physiology and Nuclear Medicine
Hvidovre Hospital
Hvidovre, Denmark
bjerregaard.fischer@gmail.com

Walther Fledelius
Post. Doc.
Oncology
Aarhus University Hospital
Århus, Denmark
walther@fledelius.com

Kirsten Fode
overlæge
onkologisk afdeling
Aarhus sygehus NBG
Aarhus c, Danmark
kirsfode@rm.dk

Lotte S Fog
Fysiker
Radiation Oncology
Copenhagen University Hospital - Rigshospitalet
Copenhagen, Danmark
lottesfog@yahoo.co.uk

Martin Fuss
MD, PhD
Department of Radiation Medicine
Oregon Health & Science University
Portland, Oregon
fussm@ohsu.edu

Karina Lindberg Gottlieb
Physicist
Laboratory of Radiation Physics
Odense University Hospital
Odense, Denmark
karina.lindberg@ouh.regionsyddanmark.dk

Cai Grau
Professor
Department of Oncology
Aarhus University Hospital
Aarhus C, Denmark
caigrau@dadlnet.dk

Vincent Gregoire
Professor in Radiation Oncology
Radiation oncology
Univ Catholique de Louvain, St-Luc Univ Hospital
Brussels, Belgium
vincent.gregoire@uclouvain.be

Anca-Ligia Grosu
Ärztl. Direktorin
Universitätsklinikum
Klinik für Strahlenheilkunde
Freiburg, Germany
anca.grosu@uniklinik-freiburg.de

Rune Groth-Hansen
Hospitalsfysiker
Afdeling for Medicinsk Fysik
Århus Sygehus
Århus C, Danmark
runegrot@rm.dk

Rasmus Hvass Hansen
MR Physicist
Dept. of Radiology
Copenhagen University Hospital, Herlev
Herlev, Denmark
rahvha01@heh.regionh.dk

Jolanta Hansen
Physicist
Dep. of Medical Physics
Aarhus University Hospital
Aarhus, Denmark
jolahans@rm.dk

Olfred Hansen
consultant
dept. oncology
Odense Universityhospital
Odense C, Denmark
olfred@dadlnet.dk

Anders Traberg Hansen
Hospital Physicist
Afdeling for Medicinsk Fysik
Århus Sygehus
Århus C, Denmark
andehans@rm.dk

David Hansen
Master Student
Institut for fysik og astronomi
Århus Universitet
Århus, Denmark
u051747@phys.au.dk

Karin Haustermans
Prof. Dr., Head of the Department
Radiation-Oncology
UZ Leuven
Leuven, Belgium
karin.haustermans@uzleuven.be

Birgitte Mayland Havelund
MD, Ph.d. student
Department of Oncology, Vejle hospital
Vejle, Denmark
birgitte.mayland.havelund@slb.regionsyddanmark.dk

Lone Hoffmann
Hospital physicist
medical physics
Aarhus University hospital
Aarhus, Denmark
lonehoff@rm.dk

Sten Hornsleth
Managing Director
Oncology Systems
Varian Medical Systems Scandinavia A/S
Herlev, Denmark
sten.hornsleth@varian.com

Michael Horsman
Associate Professor
Dept. Experimental Clinical Oncology
Aarhus University Hospital
Aarhus C, Denmark
mike@oncology.dk

Morten Høyer
Consultant
Department of Oncology
Aarhus University Hospital
Aarhus C, Denmark
hoyer@aarhus.rm.dk

Søren Haack
PhD student
Dept. of Clinical Engineering
Aarhus University Hospital
Århus N, Denmark
soeren.haack@stab.rm.dk

Lindegaard Jacob Christian
Consultant
Department of Oncology
Aarhus University Hospital
Aarhus, Denmark
jaclin@dadlnet.dk

Kirsten Legård Jakobsen
Physicist
Oncological
Herlev Hospital
Herlev, Denmark
KiLJa@HeH.RegionH.Dk

Kenneth Jensen
M.D.
Oncology
Aarhus University Hospital
Aarhus, Denmark
kennethjensen@dadlnet.dk

Robert Jeraj
Associate Professor
Medical Physics
University of Wisconsin
Madison, WI, United States
rjeraj@wisc.edu

Helle Hjorth Johannesen
Consultant
Radiology
Herlev Hospital
Herlev, Denmark
hehjjo01@heh.regionh.dk

Jørgen Johansen
Ph.D., Ass. Professor
Dept. of Oncology
Odense University Hospital
Odense, Denmark
jorgen.johansen@ouh.regionsyddanmark.dk

Jesper Kallehauge
Medical Physicist
Department of Oncology, Medical physics
Aarhus University Hospital
Århus C, Denmark
Jespkall@rm.dk

Ása Karlsdóttir
doctor
Oncology
Haukeland universitetssjukehus
Bergen, Norway
asa.karlsdottir@helse-bergen.no

Marc Kessler
Associate Professor
Radiation Oncology
The University of Michigan
Ann Arbor, USA
mkessler@umich.edu

Andreas Kjær
Prof
Endocrinology Research Section, Department of Biomedical Sciences
Panum Instituttet
København N, Denmark
andreas.kjaer@rh.regionh.dk

Marianne Knap
MD
Oncology
Aarhus University Hospital
Aarhus, Denmark
mariknap@rm.dk

Stine Korreman
Medical Physicist
Department of Human Oncology
University of Wisconsin
Madison, USA
stine.korreman@gmail.com

Brian Holch Kristensen
Chief Physicist
Oncology Dept. R / Radiation Therapy
Herlev Hospital
Herlev, Denmark
brikr@heh.regionh.dk

Philippe Lambin
Prof
Department of Radiation Oncology
MAASTRO
Maastricht, The Netherlands
philippe.lambin@maastro.nl

Yasmin Lassen
Afdelingslæge
Oncological department
Aarhus University Hospital
Aarhus, Danmark
yasmlass@rm.dk

Louise Laursen
Academic coordinator
Experimental Clinical Oncology
Aarhus University Hospital
Århus C, Denmark
louise@oncology.dk

Indira Madani
Post-doc fellow
Radiotherapy
Ghent University Hospital
Ghent, Belgium
indira.madani@ugent.be

Eirik Malinen
Section head
Department of Medical Physics
Oslo University Hospital
Oslo, Norway
eirik.malinen@fys.uio.no

Anfinn Mehus
Chief physicist
Oncology and medical physics
Haukeland University hospital
Bergen, Norway
Anfinn.mehus@helse-bergen.no

Sandy Mohamed
Research
Dept. of Oncology
Aarhus University Hospital
Aarhus C, Denmark
sanky05@hotmail.com

Lise Saksø Mortensen
phd studerende
Dep. of Experimental Clinical Oncology
Aarhus University Hospital
Århus, Denmark
lsm@oncology.dk

Hanna Rahbek Mortensen
Phd.student
Department of Oncology
Aarhus University Hospital
Aarhus C, Denmark
hanmorte@rm.dk

Per Munck af Rosenschöld
Research Physicist
Radiation Oncology
Rigshospitalet
CPH, Denmark
per.munck@rh.regionh.dk

Ludvig P Muren
Assoc prof
Dept of Medical Physics
Aarhus University / Aarhus University Hospital
Aarhus, Denmark
ludvmure@rm.dk

Søren Møller
Resident physician
Onkologisk Klinik
Copenhagen University Hospital Rigshospitalet
København Ø, Danmark
dr.smoller@gmail.com

Christian Maare
MD, ph.d.
Onkologisk Afdeling
Herelv Hospital
Søborg, Denmark
chrma@heh.regionh.dk

Jane Nielsen
Physicist
Afd.f.Medicinsk Fysik
Aalborg Sygehus Syd
Aalborg, Denmark
jan@rn.dk

Martin Nielsen
Physicist
Department of Medical Physics
Aalborg Hospital
Aalborg, Denmark
martin.skovmos.nielsen@rn.dk

Thomas Nielsen
Postdoc.
Dept. Experimental Clinical Oncology
Aarhus Universisty Hospital
Aarhus C, Denmark
thomas@oncology.dk

Tine Bjørn Nielsen
Ph.D. studerende
Syddansk Universitet
Radiofysisk Laboratorium
Odense C, Denmark
tine.bjoern.nielsen@ouh.regionsyddanmark.dk

Marianne Nordsmark
Senior staff specialist, ass. prof.
Oncology
Aarhus University Hospital
Aarhus C, Denmark
marianne@oncology.dk

Tine B. Nyeng
Medical Physicist
Dept of Medical Physics
Aarhus University Hospital
Aarhus N, Denmark
tinenyen@rm.dk

Christa Haugaard Nyhus
MD
Oncology, Vejle
Sygehus Lillebælt, Vejle
Vejle, Denmark
nyhus@pc.dk

Håkan Nyström
chief physicist
Skandionkliniken
KAS
Uppsala, Sweden
hakan.nystrom@skandion.se

Ole Nørrevang
Chief Physicist
Department of Medical Physics
Aarhus Universityhospital
Aarhus, Denmark
olenoerr@rm.dk

Birgitte Offersen
MD, phd
Dept. Oncology
Aarhus University Hospital
Aarhus, Denmark
bvo@oncology.dk

Dag Rune Olsen
Dean
Faculty of Mathematics and Natural Sciences
University of Bergen
Bergen, Norway
dag.olsen@mnfa.uib.no

Wiviann Ottosson
Medical physicist
Department of Oncology
Division of Radiophysics
Herlev, Denmark
wivott01@heh.regionh.dk

Rickard Ottosson
PhD-student
Radiation research division
Risø-DTU
Roskilde, Denmark
riot@risoe.dtu.dk

Jens Overgaard
professor
Department of Experimental Clinical Oncology
Aarhus University Hospital
Aarhus, Denmark
jens@oncology.dk

Helle Pappot
Senior medical advisor, MD, DMSc
Department of Healthplanning
National Board of Health
Copenhagen S, Denmark
hpa@sst.dk

Mike Partridge
Team Leader
Joint Department of Physics
The Inst of Cancer Res & Royal Marsden Hospital
Sutton, UK
m.partridge@physics.org

Erik Morre Pedersen
Consultant
Dept. Radiology, NBG
Aarhus University Hospital
Århus C, Denmark
erik@morrepedersen.dk

Jørgen B. Petersen
Physicist
Dept of Medical Physics
Aarhus University Hospital, Aarhus Sygehus
Aarhus C, Denmark
joerpete@rm.dk

Stine Elleberg Petersen
PhD student
Department of Oncology, Aarhus Sygehus
Aarhus University Hospital
Aarhus C, Denmark
stine@oncology.dk

Richard Poetter
Chairman
Dep of Radiotherapy,Vienna General Hospital
Medical University of Vienna
Vienna, Austria
richard.poetter@akhwien.at

Per Rugaard Poulsen
Post.doc.
Department of Oncology
Aarhus University Hospital
Aarhus, Denmark
perpolse@rm.dk

Lars Hjorth Praestegaard
Technical manager
Medical physics
Aarhus University Hospital
Aarhus, Denmark
larsprae@rm.dk

Hanne Primdahl
Physician
Department of oncology
Aarhus University Hospital
Århus, Denmark
hanpri@rm.dk

Bernt Rekstad
Medical Physicist
Department of radiation physics
Oslo University Hospital - Ullevål
Oslo, Norway
beek@uus.no

Jan Rødal
Research fellow
Dept. of Medical physics
The Norwegian Radium Hosp, Oslo Univ Hospital
Oslo, Norway
jan.rodal@radiumhospitalet.no

Kathrine Røe
PhD student
Radiation Biology
Institute for Cancer Research, Oslo Univ Hospital
OSLO, Norway
Kathrine.Roe@rr-research.no

Lisbeth Røhl
Konstitueret overlæge PhD
Radiologisk afdeling
Århus Sygehus NBG
Århus C, Denmark
lisbeth_rohl@hotmail.com

Heidi S. Rønde
Medical physicist
Department of Medical Physics
Vejle Hospital
Vejle, Denmark
Heidi.Staghoej.Roende@slb.regionsyddanmark.dk

Annette Schouboe
radiotherapist
d-terapi, onkologisk afdeling
Århus sygehus
Århus C, Denmark
annescho@rm.dk

Henrik Schultz
consultant oncologist
Oncology
Aarhus University Hospital
Aarhus, Denmark
heschu@rm.dk

Peter Sandegaard Skyt
PhD student
Department of Medical Physics
Aarhus University Hospital
Aarhus, Denmark
skyt@phys.au.dk

Thea Sollien
Student
Department of Medical Physics
Oslo University Hospital
Oslo, Norway
theaso@student.uio.no

Rune Sylvarnes
Medical Physicist
Cancer department
University Hospital of North Norway
Tromsø, Norway
Rune.Sylvarnes@unn.no

Jimmi Søndergaard
Ph.d. student
Oncology
Aarhus University Hospital
Aarhus, Denmark
jimmsoen@rm.dk

Christian Søndergaard
Physicist
Department of Medical Physics
Aarhus University Hospital
Aarhus, Denmark
chrissnd@rm.dk

Thomas Sangild Sørensen
Associate Professor
Dept. Computer Science and Inst. Clinical Medicine, Aarhus University
Århus N, Denmark
sangild@cs.au.dk

Åste Søvik
Research scientist
Department of Medical Physics
Norwegian Radium Hospital, Oslo Univ Hospital
Oslo, Norway
aste@fys.uio.no

Kari Tanderup
Post.Doc
Dept. of Oncology
Aarhus University Hospital
Aarhus C, Denmark
karitand@rm.dk

Mette Skovhus Thomsen
medical physicist
Medical Physics
Aarhus University Hospital
Århus C, Danmark
mette.skovhus.thomsen@aarhus.rm.dk

Maria Thor
PhD student
Departments of Oncology and Medical Physics
Aarhus University Hospital
Århus C, Denmark
mariathor84@gmail.com

Ester Holm Thøgersen
Radiographer
Med. fys.
Aarhus
Aarhus C, Denmark
ester.radiograf@aarhus.rm.dk

Sara Thörnqvist
Ph.d-student
Dep. of Medical physics
Aarhus University Hospital
Århus, Danmark
sara.thornqvist@gmail.com

Iuliana Toma-Dasu
Assistant Professor
Medical Radiation Physics
Stockholm University and Karolinska Institutet
Stockholm, Sweden
Iuliana.Livia.Dasu@ki.se

Silke Ulrich
Postdoc
Department of Radiation Oncology
Rigshospitalet
Copenhagen, DK
silke80@gmx.de

Niels Ulsø
Past Medical Physicist
Department of Oncology
Aarhus University Hospital
Risskov, Denmark
niels@nac.dk

Uulke van der Heide
Medical Physicist
Radiotherapy
University Medical Center Utrecht
Utrecht, The Netherlands
u.a.vanderheide@umcutrecht.nl

Silvia Vargas Castrillon
Senior Researcher
Lab de Metrología de Radiaciones Ionizantes
CIEMAT
Madrid, Spain
silvia.vargas@ciemat.es

Anne Vestergaard
Medical Physicist
Dep. of Medical Physics
Århus University Hospital
Århus, Denmark
annveste@rm.dk

Ivan Storgaard Vogelius
Medical Physicist
Finsencentret
Rigshospitalet
Nørresundby, Denmark
vogelius@gmail.com

Michael Væth
Professor
Biostatistics
University of Aarhus
Århus C, Denmark
vaeth@biostat.au.dk

Lennart Ward
Business Unit Manager
Nordic BU
Elekta Instrument AB
Stockholm, Sweden
lennart.ward@elekta.com

Petra Witt
MD, PhD
Department of Oncology
Uppsala University Hospital
Uppsala, Sweden
pmwa@dadlnet.dk

Esben Worm
Medical Physicist
Medical Physics
Aarhus University Hospital
Aarhus C, Denmark
esbeworm@rm.dk

Pauliina Wright
PhD student
Medical Physics
Aarhus Univ Hosp and The Norwegian Radium Hospital, Oslo, Norway
paulwrig@rm.dk

John Yarnold
Professor of Clinical Oncology
Academic Radiotherapy Department
The Royal Marsden NHS Foundation trust
Sutton, UK
John.Yarnold@icr.ac.uk

Christina Zacharatou,
Medical physicist
Radiation Oncology
Rigshospitalet
Copenhagen, Denmark
christina.zacharatou@cern.ch